

# Geophysical, isotopic, and hydrogeochemical tools to identify potential impacts on coastal groundwater resources from Urmia hypersaline Lake, NW Iran

Vahab Amiri<sup>1</sup> · Mohammad Nakhaei<sup>1</sup> · Razyeh Lak<sup>2</sup> · Majid Kholghi<sup>3</sup>

Received: 29 December 2015 / Accepted: 9 May 2016 / Published online: 17 May 2016  
© Springer-Verlag Berlin Heidelberg 2016

**Abstract** Measurements of major ions, trace elements, water-stable isotopes, and geophysical soundings were made to examine the interaction between Urmia Aquifer (UA) and Urmia Lake (UL), northwest Iran. The poor correlation between sampling depth and  $\text{Cl}^-$  concentrations indicated that the position of freshwater-saltwater interface is not uniformly distributed in the study area, and this was attributed to aquifer heterogeneities. The targeted coastal wells showed B/Cl and Br/Cl molar ratios in the range of 0.0022–2.43 and 0.00032–0.28, respectively. The base-exchange index (BEI) and saturation index (SI) calculations showed that the salinization process followed by cation-exchange reactions mainly controls changes in the chemical composition of groundwater. All groundwater samples are depleted with respect to  $\delta^{18}\text{O}$  (–11.71 to –9.4‰) and  $\delta\text{D}$  (–66.26 to –48.41‰). The  $\delta^{18}\text{O}$  and  $\delta\text{D}$  isotope ratios for surface and groundwater had a similar range and showed high deuterium excess (d-excess) (21.11 to 31.16‰). The high d-excess in water samples is because of incoming vapors from the UL mixed with an evaporated moisture flux from the Urmia mainland and incoming vapors from the west (i.e., Mediterranean Sea). Some saline samples with low B/Cl and Br/Cl ratios had depleted  $\delta^{18}\text{O}$  and  $\delta\text{D}$ . In this

case, due to freshwater flushing, the drilled wells in the coastal playas and salty sediments could have more depleted isotopes, more  $\text{Cl}^-$ , and consequently smaller B/Cl and Br/Cl ratios. Moreover, the results of hydrochemical facies evolution (HFE) diagram showed that because of the existence fine-grained sediments saturated with high density saltwater in the coastal areas that act as a natural barrier, increasing the groundwater exploitation leads to movement of freshwaters from recharge zones in the western mountains not saltwater from UL. The highly permeable sediments at the junction of the rivers to the lake are characterized by low hydraulic gradient and high hydraulic conductivity. These properties enhance the salinization of groundwater observed in the study area. The main factors influencing the salinity are base-exchange reactions, invasion of highly diluted saltwater, dissolution of salty pans, and water chemistry evolution along flow paths.

**Keywords** B/Cl · Br/Cl · Stable isotopes · Freshwater-saltwater interface · Urmia Aquifer

## Introduction

The management of fresh groundwater resources is an increasingly important imperative for the custodians of natural resources. Freshwater stored in coastal aquifers is particularly vulnerable to degradation due to its nearness to salt water, in combination with the intensive water demands that accompany higher population densities of coastal zones. Future exploitation of groundwater in the Middle East, for example, and in many other water-scarce regions in the world depends largely on the degree and rate of salinization (Vengosh and Rosenthal 1994; Vengosh et al. 2001; Ranjan et al. 2006; Sowers et al. 2011; Madani 2014). Salinization is a global environmental

Responsible editor: Philippe Garrigues

✉ Vahab Amiri  
vahab.amiri@gmail.com

<sup>1</sup> Department of Applied Geology, Faculty of Earth Sciences, Kharazmi University, Tehran, Iran

<sup>2</sup> Research Institute of Earth Sciences, Geological Survey of Iran, Tehran, Iran

<sup>3</sup> Department of Irrigation and Reclamation Engineering, Faculty of Agriculture and Natural Resources, University of Tehran, Tehran, Iran

phenomenon that affects diverse aspects of our lives: changing the chemical composition of natural water resources, degrading the quality of water supplied to domestic and agriculture sectors, affecting ecological systems by loss of fertile soil, resulting in collapse of agricultural and fishery industries, changing local climatic conditions, and creating severe health problems (Jackson et al. 2001; Williams 2001a,b; Dregne 2002; Williams et al. 2002; Rengasamy 2006).

The most relevant salt sources/processes recognized worldwide are: evaporation, evaporite leaching, mobilization of salts stored in the unsaturated zone, infiltration of non-marine-polluted surface waters, slow-moving saline/salt waters of marine, lake, and lagoon origin (Darling et al. 1997; Barbecot et al. 2000), highly mineralized waters from hydrothermal igneous activities (Fidelibus et al. 2011), sea spray, membrane effects (salt filtering, hyper-filtration, or reverse osmosis), agricultural practices (return flow, use of fertilizers and irrigation with treated wastewater), cycling wetting, and drying.

The salinity problem is only the “tip of the iceberg” as high levels of sodium and chloride can be associated with high concentrations of other inorganic contaminants such as sulfate, boron, fluoride, and bio-accumulated elements such as selenium and arsenic. The salinization process may also enhance the mobilization of toxic trace elements in soils due to competition of ions for adsorption sites and formation of metal-chloride complexes (Backstrom et al. 2003, 2004) and oxyanion complexes (Amrhein et al. 1998; Goldberg et al. 2008). Thus, the chemical evolution of the major dissolved constituents in a solution will determine the reactivity of trace elements with the host aquifer/streambed solids and, consequently, their concentrations in water resources.

Increasing demands for water have created tremendous pressures on water resources as overexploitation that have resulted in the lowering of groundwater levels (causing lateral saline/saltwater intrusion and/or upconing) and consequently increasing salinization. In many aquifers in Iran, for example, salinity is the main factor that limits water utilization, and future prospects for water use are complicated by increasing salinization (Jalali 2007; Samani and Asghari Moghaddam 2015; Amiri et al. 2015).

Understanding the hydrologic connection among groundwater systems is critical for developing sustainable groundwater-management strategies. When hydrogeologic data is insufficient to determine the degree of interaction between surface and groundwater systems (for example in this study between UA and UL), hydrogeochemical indicators (Wahi et al. 2008; Manning 2009; Musgrove et al. 2010; Gardner and Kirby 2011), water-stable isotopes (Gaye 2001; Trabelsi et al. 2012; Mongelli et al. 2013; Skrzypek et al. 2013; Sprenger et al. 2015), and geophysical surveys (Wilson et al. 2006; Morrow et al. 2010;

Kouzana et al. 2010; Zarroca et al. 2011; Asfahani and Abou Zakhem 2013) can be used to assess the connection.

The present study has been carried out within the Urmia Aquifer (UA), next to the Urmia Lake (UL). This lake, one of the largest hypersaline lakes of the world, is located in northwest of Iran. It is a natural asset with considerable ecological, environmental, and cultural values. UL is a National Park and has been recognized by UNESCO as a Biosphere Reserve. For the last decade, UL has been in a critical condition because of declining water levels and increasing salinity (Ministry of Energy of Iran 2010). There is considerable evidence that groundwater resources are already being exploited at rates faster than aquifer recharge in the area of the UL watershed (Wada et al. 2010; Zarghami 2011).

This study attempts to describe: (a) processes and degree of the saltwater encroachment, (b) mechanisms in terms of salinization or freshening, and (c) other possible factors that may have impact in the salinity of the UA. Major ions chemistry in groundwater are of incomplete value to determine the three subjects mentioned above, but still are worthwhile in ascertaining parameters for saltwater encroachment because they can be readily obtained by routine groundwater analyses. In addition to the major ions, like some new studies, we used the minor elements (e.g., bromide and boron) to define source(s), mixing rates, and salinization mechanisms in the Urmia groundwater resources. These constituents are used as makers for the source of salinity and salinization processes in the UA. Water-stable isotopes ( $\delta^{18}\text{O}$  and  $\delta\text{D}$ ) also are used for associate evidence of mentioned processes. In this study, a geophysical survey based on the Vertical Electrical Sounding (VES) Schlumberger configuration was carried out in the coastal parts of the UA to improve the knowledge of the aquifer, to detect the potential salinity at the UL ward boundary of aquifer, and to determine the character and dynamics of the saline interface. Finally, the salinization cross-sections in normal directions to the coastline are presented to determine the salinization conditions in this aquifer.

## Materials and methods

### Study area

Our study area is in the northwest of Iran. This region is located between the eastern longitude of  $44^{\circ}$ ,  $20'$  and  $45^{\circ}$ ,  $20'$  and northern latitude of  $37^{\circ}$ ,  $05'$  and  $38^{\circ}$ ,  $05'$  (Fig. 1). This region with approximately  $4268\text{ km}^2$  in area has the altitude in range of 1280 and 3608 above mean sea level. Groundwater resources in UA are very important sources of water. The UA has a large storage capacity, regulating the inflow and outflow from a significant drainage area. The thickness of UA varies from a few meters to near 170 and 130 m in northern and southern parts of aquifer, respectively.

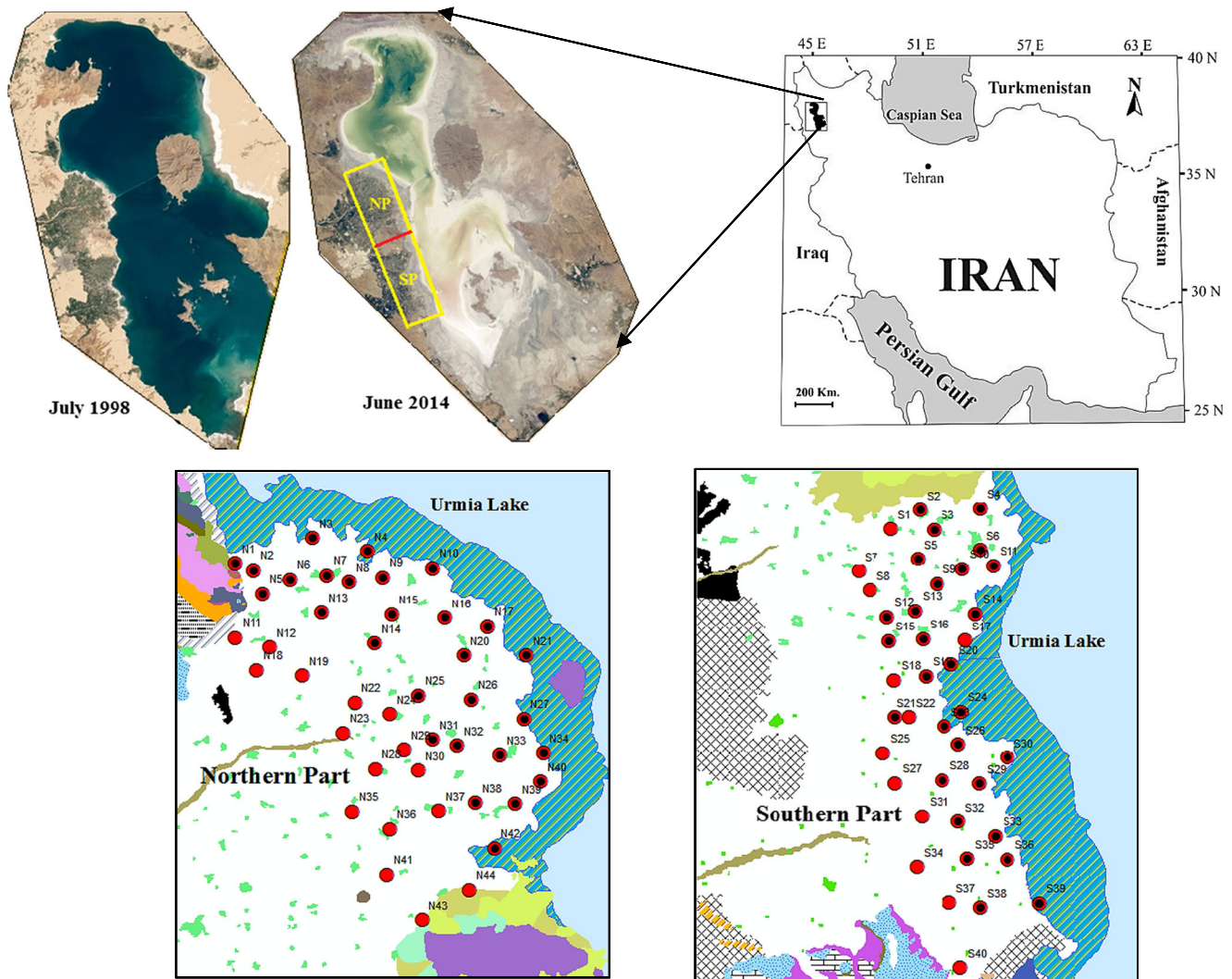


**Fig. 1** Location of the different selected sampling sites in the UA. The dramatic reduction in water level and area of UL between July 1998 and June 2014 is displayed (Satellite images: Kaveh Madani). *Red and black*

*points* are the groundwater samples collected in June 2014 and September 2014, respectively. The water sampling in May 2015 for isotopic and hydrochemical analysis is done in this sampling network

The groundwater flow direction is from west to east (UL). Hydrological investigations have shown that this aquifer spreads under an area of approximately 868 km<sup>2</sup> and consists of confined and unconfined aquifers (Badv and Deriszadeh 2005). The major sources for recharging the UA are four perennial rivers, including Nazlou-chai, Rowzeh-chai, Shahr-chai, and Barandouz-chai, which are flowing in the plain. These rivers originate from the western mountains and end in UL. The mean input to the aquifer from these rivers and return flows from irrigated lands is about 290 million cubic meters (MCM) per year. In addition, infiltration from precipitation is near 37.7 MCM per year. In this area, the irrigation is mainly from groundwater sources (Mohammadi 2012).

The oldest rock units of the Pre-Cambrian are formed by meta volcanic series, acidic tuff, and diorite in the surrounding mountains of UA, as well as metamorphous amphibolites and gneiss. In this area, the Ophiolite units consist of basic and

ultra-basic rocks with schist and radiolarite limestone. Tertiary rocks in this plain are represented by limestone, conglomerate, sandstone, and shale (Kamei et al. 1973).

This area is in a Mediterranean pluvial seasonal-continental climate, as stated by the Global Bioclimatic Classification System (Martinez et al. 1999). During the recent 30-year period, mean annual temperature and precipitation in the area are 11.52 °C and 346.3 mm, respectively, while mean maximum and minimum temperatures occur in July (31.2 °C) and January (−6.1 °C), respectively (NOAA 2012; WMO 2014).

The UA is located in the east of UL. In this lake, salinity has been increasing over the recent years (from 166 g/l in 1995 to over 412 g/l in 2015) due to reduction in precipitation, the overexploitation of water for agricultural purposes, and the construction of dams to supply potable water to the residential sector (Khatami 2013). In the past 20 years, UL's water level has dropped by more than 7.84 m, and it was about 1270.07 m

above mean sea level in October 2015. The water fluctuation for the past 38 years and a picture from present state of UL is represented in Fig. 2.

### Water sampling and analyses

To assess the present state of UA, water samples were collected during three sampling periods (June 2014, September 2014, and May 2015). In this study, 84, 57, and 42 wells regularly distributed over the coastal area were considered to sampling in June 2014, September 2014, and May 2015, respectively. Most of the wells are used for irrigation and industrial and, in some cases, for drinking purposes. Water samples were collected from shallow and deep boreholes and hand dug wells ranging in depth from 10 to 120 m using standard sampling procedures (APHA 1985; ISO 5667-11 1993). Sampling points always coincide in the three periods, and there was a homogeneous distribution of water samples over the aquifer. Water samples were collected from pumping wells after minimum of several hours of pumping prior to sampling in order to remove any standing water from the wells. At each sampling point, samples were stored in two 250-ml polyethylene bottles after being filtered through 0.45- $\mu\text{m}$  membrane filters and were divided into two groups: (1) filtered non-acidified for anion analysis and (2) filtered acidified (with a few drops of Suprapur<sup>®</sup> nitric acid ( $\text{HNO}_3$ , 65 % v/v; Merck, Germany)) for cation analysis. At each sampling point, Eh, pH, T, salinity, dissolved oxygen (DO), and electrical conductivity (EC) parameters were measured in the field using a HACH Multimeter device (HACH, Germany). The collected samples were kept in an ice box and then transferred to a fridge where they were stored at 4 C until delivery to the laboratory for analyses. The concentrations of chemical parameters in water samples were analyzed by Zarazma Mineral Studies Company (ZMSC) Ltd. in Tehran, Iran, utilizing inductively coupled plasma-mass spectrometry (ICP-MS) (Model-Quadrupole, High Performance, 4500) for  $\text{Ca}^{2+}$ ,  $\text{Mg}^{2+}$ ,  $\text{Na}^+$ ,  $\text{K}^+$  cations and B, ion chromatography for  $\text{Br}^-$  (method ref. APHA 4110B), discrete analyzer in water by Aquakem DA for

$\text{SO}_4^{2-}$  and  $\text{Cl}^-$  anions (method ref. APHA 4500), and  $\text{HCO}_3^-$  alkalinity by acid titration (method ref. APHA 2320). Calibration of ICP-MS was performed using NIST 1640 (National Institute of Standards and Technology, USA). Also, in this study, 47 water samples (42 samples from coastal groundwater, 3 samples from perennial rivers, and 2 samples from northern and southern parts of UL) were analyzed for stable isotope composition ( $\delta^{18}\text{O}$  and  $\delta\text{D}$ ). The stable hydrogen and oxygen isotope compositions of water samples were determined utilizing a Los Gatos Research (LGR) Liquid Water Isotope Analyzer (OA-ICOS T-LWIA) at the Environmental Isotopes Laboratory, University of Waterloo, Canada. Standards used are the Vienna Standard Mean Ocean Water (VSMOW) (Gonfiantini 1978). Analytical uncertainties are 0.22 ‰ for  $\delta^{18}\text{O}$  and 0.63 ‰ for  $\delta\text{D}$ .

## Results and discussion

### Geophysical assessment of coastal areas

A careful analysis of the literature indicates that the continuity of the assemblage of aquifer units from the onshore areas to inner areas is almost unknown. In this study, we attempted to determine the subsurface sedimentary/rock units, especially in the coastal area of the aquifer, based on data collected from geological formations, previous studies, and field observations. In the present research, VES data collection was directed in one survey which took place at the start of intensive exploitation of the UA during summer 2014. Change in electrical resistance was attributed to various lithological units in the Urmia area (Table 1).

The variation from freshwater to saline/saltwater can be easily determined by using electrical resistivity techniques (Wilson et al. 2006; Koukadaki et al. 2007; Duque et al. 2008). In this study, four N-S geoelectric cross-sections at the east of UA (i.e., next to UL) are considered to evaluate the potential impacts on groundwater resources from UL (Fig. 3).



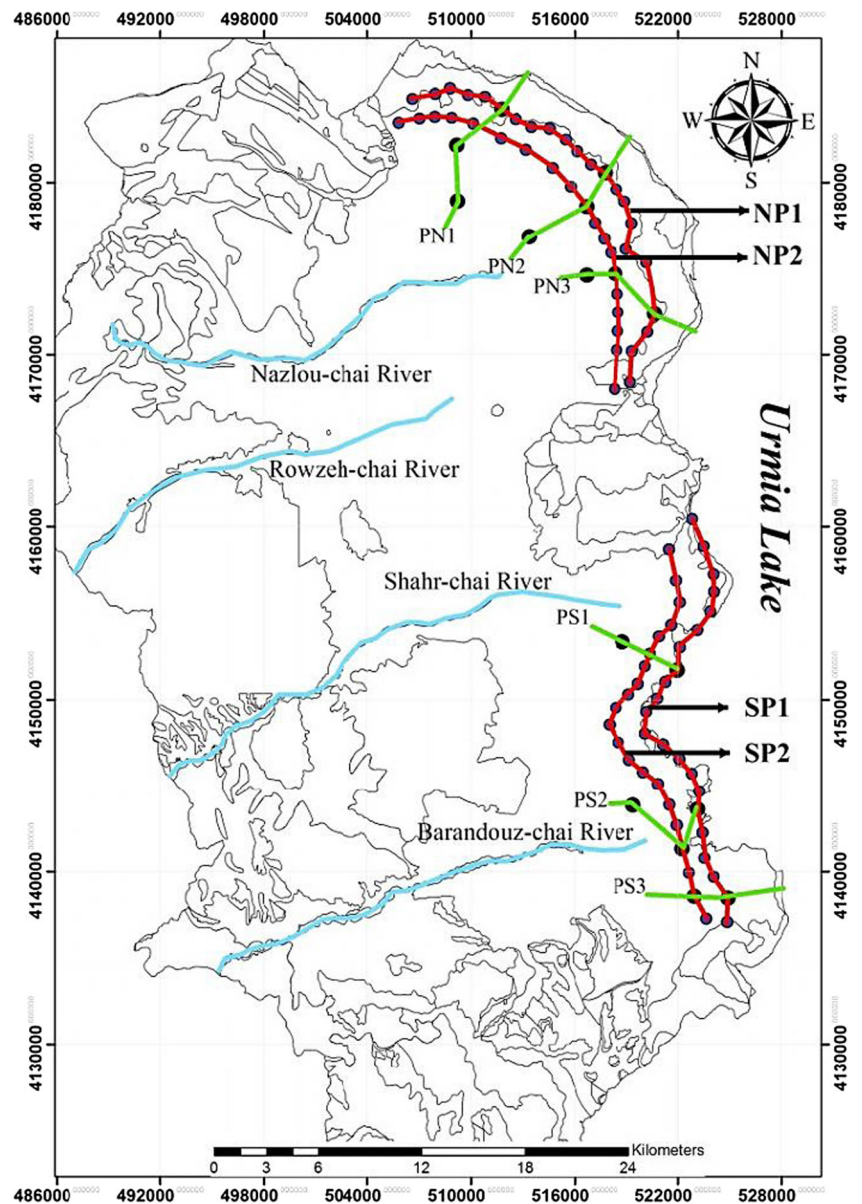
**Fig. 2** Changes in water level of UL, 1977 to 2014 (left), and the present state of water level in the Lake (right)

**Table 1** Variations of electrical resistivity for different lithological units in the Urmia area

Lithology	Bulk electrical resistivity, $\rho$ ( $\Omega$ m) (for sounding points)	Electrical resistivity, $\rho$ ( $\Omega$ m) (for cross-sections)
Clay with salt sediment/water content	<5	<5–10
Clay with some sand	5–20	10–20
Medium sand	20–30	20–30
Coarse sand	30–60	30–100
Coarse sand with gravel	>60	>100
Bedrock	Electrical conductive	<10
	Marl, sandstone, etc.	10–20
	Electrical resistant (e.g., volcanic rocks)	>30

The geoelectric sections for northern and southern parts of UA are presented in Fig. 4. As shown, high resistivity values were recorded at the north end of the area (see Fig. 4a). These can be attributed to the presence of high resistivity formations

**Fig. 3** The VES and profiles parallel (NP1, NP2, SP1, and SP3) and normal (PN1, PN2, PN3, PS1, PS2, and PS3) to the shoreline



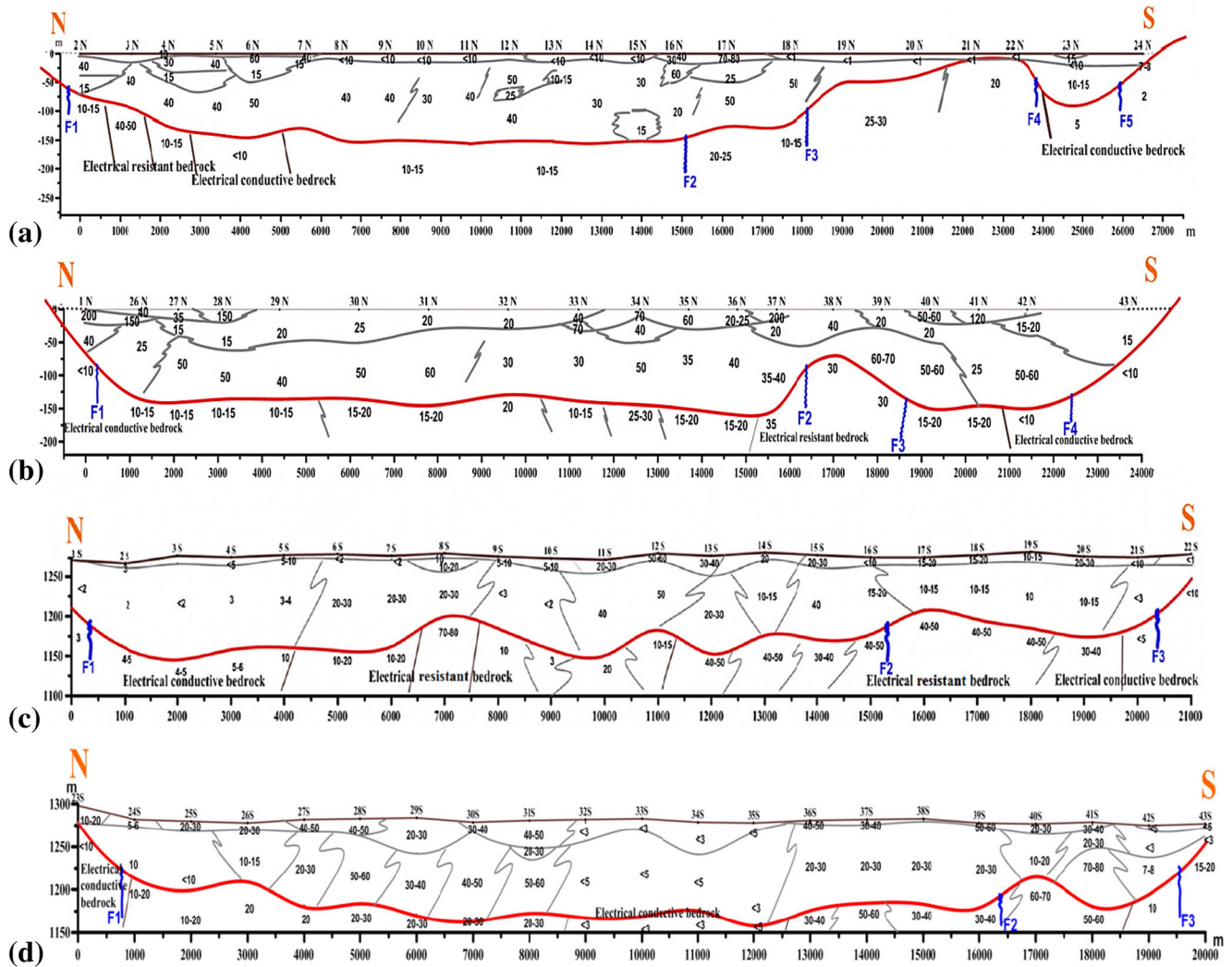


**Fig. 4** The geoelectric sections, of North-South direction, for **a, b** northern and **c, d** southern parts of UA. These sections display the subsurface structures of UA in the possible closest distance from the UL. In this figure, **a** and **b** are NP1 and NP2 and **c** and **d** are SP1 and

SP2, respectively. The average direct distance between NP1 and NP2 and SP1 and SP2 is 1700 and 2000 m, respectively. *Red line* is the boundary between alluvium and bedrock, *blue line* is the possible fault or contact, and *gray line* is the boundary between different alluvial layers

corresponding to coarse-grained sediments originated from volcanic and metamorphic rocks. Also, sediments saturated by freshwater show the high values of resistivity. Additionally, unsaturated surficial sediments and present and old flowing paths of rivers associated with the deposition of coarse-grained particles have high resistivity values (6 N, 7 N, 16 N, 17 N in NP1 and 8S, 11S-13S, 15S in SP1). Low resistivity values occur mainly in the southern half of the coastal strip area (between sounding points 1S to 5S, 9S and 10S, 21S and 22S). Therefore, it may indicate the existence of sediments (regardless of the grain size) with high salt content (as dissolved or deposited) (see Fig. 4b). Generally, in the coastal areas, sands saturated with brackish water and fine sediments rich in salts (saturated or unsaturated) present an analogous geoelectrical behavior, characterized by low bulk resistivity (Zarroca et al. 2011).

As shown in Fig. 4a, the lowest resistivity values (10–15 Ω m) in saturated porous medium of northern part are recorded in depth 100–150, 50, and 50–100 m below land surface at the sounding points 15 N and 13 N, 23 N, respectively, which suggests the fine- and medium-grained (e.g., clay and sand) sedimentary lens. The resistivity decreased to the southern part, suggesting higher salinity and/or more fine-grained sediments than in the northern part. It should be noted that low resistivity values in the surficial sediments (low depths) are because of salty pans in the near shore areas.

Assessment of inland profiles, NP2 and SP2, indicates that sedimentary basin is laterally uniform, and there is no sharp variation in sediment types. As displayed in Fig. 4, the resistivity values of surficial sediments increase with increasing distance from the UL. In addition to salty pans in the coastal areas, the groundwater level in coastal wells is higher than

inland wells (an unsaturated zone with low thickness); therefore, the capillary effect can raise the groundwater in the fine-grained sediments (unsaturated area) and more decreases the resistivity than inland sediments.

As shown in Fig. 4d, a low resistivity anomaly is observed in the central sector of the profile (between sounding points 32S–36S). Low resistivity occurs in the intermediate unit ( $<3\text{--}5\ \Omega\ \text{m}$ ), indicating that these sediments should be saturated in salt or brackish water, given the typical resistivity value for saltwater ( $0.2\text{--}0.3\ \Omega\ \text{m}$ ). In this area, field observations and measured hydrochemical parameters in extraction wells showed that the groundwater samples have EC values between 400 and 1500  $\mu\text{S}/\text{cm}$ . Very low resistivity values are because of very fine-grained particles in the area. Results shows that UA has low permeability in this area. In addition, groundwater will overflow (i.e., artesian) by increasing the depth of wells to more than 100 m below the land surface. The surrounding units offer resistivity values significantly higher ( $20\text{--}50\ \Omega\ \text{m}$ ). These sediments encompass lower fluid salinity, corresponding to fresh or slightly brackish water. Furthermore, their bulk resistivity decreases smoothly towards the coastline to values below  $20\ \Omega\ \text{m}$ . Given these contradictions, detailed geophysical studies should be conducted to determine the precise limits of this area.

In addition to the cross-sections parallel to the coastline described above, we tried to assess the possible impact of UL on groundwater resources by examining of resistivity changes in depth for some profiles perpendicular to the coastline. Agricultural development and some constructions in the study area constrained the location of some VES, and thus, the sounding points could not be located in the exact same position of pumping wells. However, 16 sounding points were used with an acceptable degree of concordance with nearest extraction wells in order to assess the salinization issue (see Fig. 4 and Table 2). These points were selected based on their most variations in chemical composition and electrical resistivity during the sampling and study processes (June 2014 to May 2015).

As presented in Table 2, six resistivity profiles are considered in this area. Each profile is composed of 2–3 sounding points (i.e., A, B, C). In these profiles, point A is located at the nearest distance to the UL and point C at the inland areas. Locations of profiles are shown in Fig. 3. The corresponding extraction wells for these sounding points are presented in Table 2. Some parameters such as well depth,  $\text{Cl}^-$  concentration, salinity, EC, and pH are also measured.

The resistivity and EC patterns in the northern and southern parts of UA shown in Fig. 5 are different. The patterns in the southern part are remarkably similar. Most profiles in the northern part show a resistivity increase in low depths (unsaturated soils) and then smooth reduction in more depths. In contrast, the profiles in the southern part show a decrease in resistivity

for surficial layers and then an increase in greater depths.

Profile PN1 (A-C) is located at the north of area. As shown in Fig. 5a, resistivity values in PN1-A (near shoreline) are lower than inland sounding points (PN1-B and PN1-C). The slow increase in electrical resistivity is because of the unsaturated surficial sediments. The critical depth to reduce the resistivity in different points is between 8 and 40 m below land surface. In this study, a simplified equation is used to convert bulk resistivity (in  $\Omega\ \text{m}$ ) to electrical conductivity (EC, in  $\mu\text{S}/\text{cm}$ ). The real values of EC and other hydrochemical parameters for three wells (N4, N8, and N13) at the sounding locations are presented in Table 2. Given the high values of  $\text{Cl}^-$  and EC in the UL saltwater, chloride concentrations greater than 150 and 1000 mg/l were considered as an evidence for fresh brackish and brackish-salt water mixing with freshwater in the aquifer and indicate the presence of the saltwater interface (i.e., diluted saltwater). Resistivity data for point PN1-A show a decrease in depth 40 m below land surface. Nearby well N4 with depth 45 m had a chloride concentration of about 145 mg/l in September 2014. The results clearly indicate that the estimated EC values (Fig. 5g) using mentioned relation are lower than real measurements. It is due to saturated fine sediments in this area and ignoring other effective factors (e.g., groundwater resistivity, formation factor, and temperature correction of groundwater resistivity) in the relation.

Profile PN2-(A-C) (Fig. 5b, h) is located in the flowing direction of Nazlou-chai river. Therefore, it is expected that this area be covered with high resistivity sediments. This area particularly at the coastline (for instance in PN2-A) is prone to saltwater intrusion because of the decline in groundwater level, reduction of river discharge, and increase in UL level. The results show that measured EC values in three production wells nearby the sounding points increased from inland (well N25;  $\text{EC}=810\ \mu\text{S}/\text{cm}$ ,  $\text{Cl}^-=31\ \text{mg}/\text{l}$ ) to the shoreline (well N17;  $\text{EC}=5600\ \mu\text{S}/\text{cm}$ ,  $\text{Cl}^-=750\ \text{mg}/\text{l}$ ) areas. Figure 5h indicates that estimated EC value in PN2-A decreases with increasing depth. Given the depth of well N17 (i.e., 17 m), it can be concluded that salinity of this well is not due to the direct influence of UL and the main reason for this phenomenon is the dissolution of salt pans. Resistivity patterns and estimated EC values for profile PN3-(A-C) (Fig. 5c, i) are similar to profile PN2-(A-C). The highest values of EC and  $\text{Cl}^-$  in this profile are observed in well N34 ( $\text{EC}=2320\ \mu\text{S}/\text{cm}$ ,  $\text{Cl}^-=385\ \text{mg}/\text{l}$ ). In this profile, there is no evidence for saltwater intrusion in more depths.

In some areas of southern part (e.g., central areas), shallow groundwaters (depth  $<40\ \text{m}$ ) generally have more EC than deep groundwaters (depth  $>60\ \text{m}$ ). In other words, with increasing depth and passing through a discontinues saturated and relatively compacted clayey layer, low EC groundwater flows out on to the ground surface (i.e., artesian system). Therefore, we can consider UA, particularly at the central

**Table 2** Summary of geoelectrical points at the nearest groundwater sampling wells in the UA. Data are collected in September 2014

Profile ID	Part	VES point	Sampling well	Well depth	Cl <sup>-</sup> (mg/l)	Salinity (‰)	EC (μS/cm)	pH
PN1	A	7 N	N4	45	145	0.71	1430	7.08
	B	47 N	N8	40	40	0.72	1444	7.43
	C	87 N	N13	35	55	0.83	1670	7.01
PN2	A	14 N	N17	17	750	2.8	5600	7.60
	B	34 N	N20	12	55	0.84	1750	7.28
	C	68 N	N25	60	31	0.4	810	7.52
PN3	A	20 N	N34	50	385	1.16	2320	8.77
	B	38 N	N33	16	33	0.34	750	7.50
	C	55 N	N32	18	20	0.41	818	7.33
PS1	A	8S	S14	68	33.5	0.25	503	7.85
	B	50S	S13	50	14	0.38	765	7.33
PS2	A	17S	S30	10	2061.4	3.6	7180	7.21
	B	40S	S29	30	45	0.65	1305	7.35
	C	58S	S28	120	11	0.25	510	7.72
PS3	A	21S	S39	86	170	0.68	1370	7.87
	B	62S	S38	100	30	0.52	1045	7.48

and near shore areas of southern part, as a convertible unconfined/confined system. This phenomenon could also be observed in some areas close to the coast of the northern part. In the southern part, the mentioned system is observed particularly at the central and southern areas. The present conditions could be explained with reference to the presence of fine-grained sediments of lake in the deep coastal areas, the impossibility of groundwater flow beneath the UL due to high-density brines, and thus hydrostatic pressure increase within the aquifer. The highest values of EC and Cl<sup>-</sup> in the southern part (EC = 7180 μS/cm, Cl<sup>-</sup> = 2061.4 mg/l) have been recorded in well S30, corresponding to sounding point 17S (PS2-B) (Fig. 5e, k). Well S39 near sounding point 21S in profile PS3 (PS3-A) is artesian. This well showed EC = 1370 μS/cm and Cl<sup>-</sup> = 170 mg/l in September 2014 (during geoelectrical study). The field observations revealed that the shallow groundwater in this point is saline (EC = 2990 μS/cm, Cl<sup>-</sup> = 498.7 mg/l). Therefore, our findings in this regard indicate that the salinity in shallow and deep groundwaters is not due to direct intrusion of UL saltwater.

**General water characteristics**

In three wet and dry seasons, the groundwater samples had average temperatures during sampling of around 15.7 to 20 °C, reflecting that they are higher than the average yearly temperature of the study area. In the wet seasons (June 2014 and May 2015), the pH values change from 6.95 to 8.27 and Eh values from -106.28 to 4.84 mV. In the dry season (September 2014), pH and Eh values range between 6.98 to 8.92 and -88 to 0.6 mV, respectively. In the wet seasons, EC varied considerably from 355 to 5853 μS/cm and in the dry

season changes from 428 to 7180 μS/cm. Figure 6 presents the EC values of the groundwater samples in June 2014 and September 2014. In UL; the average values of EC range between 130.8 and 189.94 mS/cm for wet and dry seasons, respectively. During this period, the pH values change from 6.35 to 6.60.

**UL saltwater intrusion**

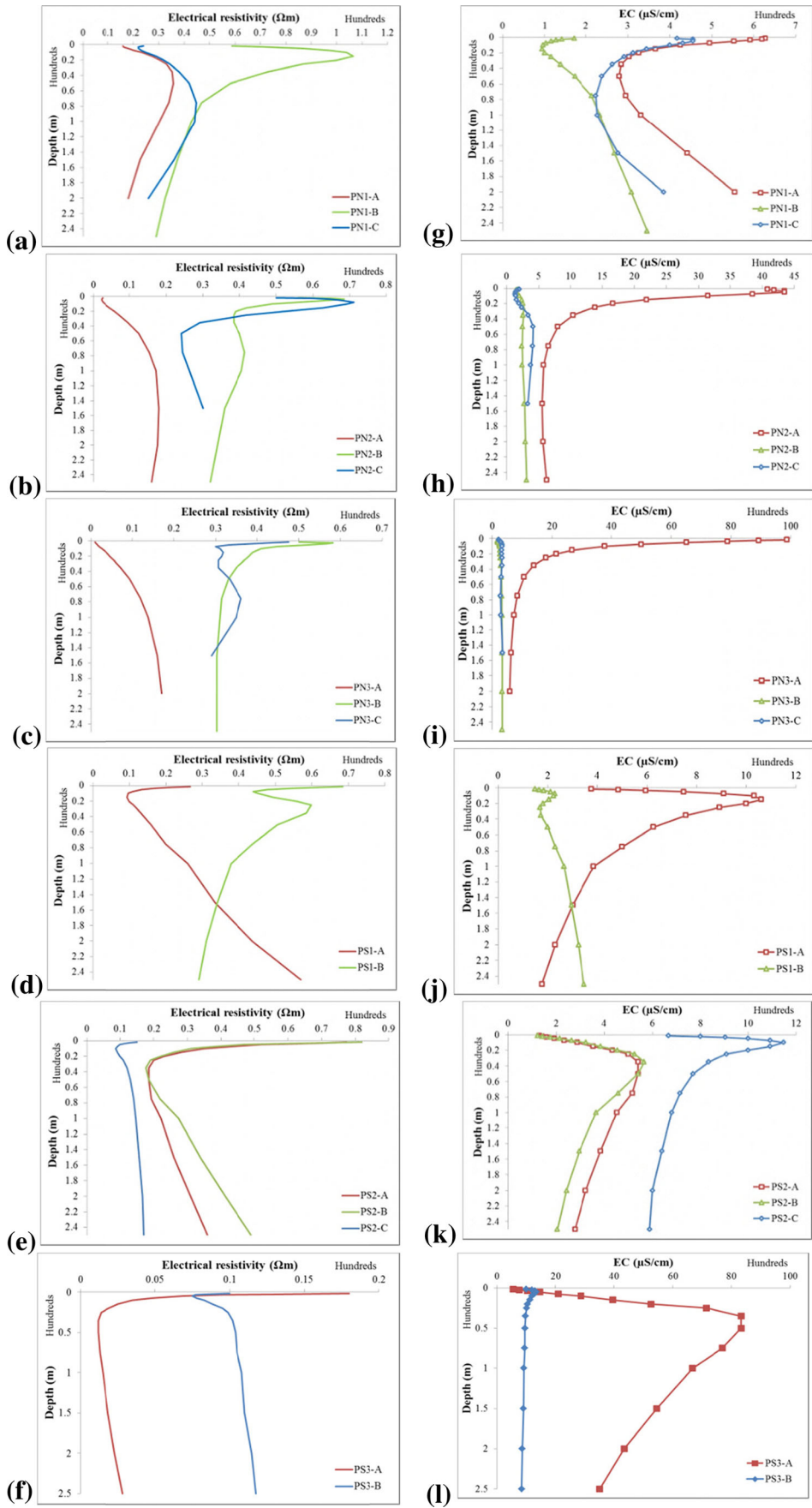
In an attempt to delineate the sources and mechanisms of groundwater salinization in a under risk coastal aquifer, one can define two types of geochemical tracers (T1, T2) that are capable of delineating the three principal saline sources:

*Conservative elements ratios*

T1 type tracers include some ion ratios, particularly the ratios of conservative elements such as Br/Cl and B/Cl. These tracers are used to identify the dissolution of salts and mixing with external groundwaters. These tracers cannot be used to identify evaporation process in the aquatic environment (Vengosh 2014). Based on the previous studies, there are different sources of bromide, boron, and chloride in water samples and, consequently, various B/Cl and Br/Cl ratios (Table 3).

**Fig. 5 a–f** Measurements of bulk electrical resistivity (in Ω m) as a function of depth, and **g–l** changes of estimated EC (= (1/ρ) × 10,000) based on collected VES data along 6 profiles (including 16 sounding point) in the northern and southern parts of aquifer. PN (or PS)-A (red lines) is the nearest point and PN (or PS)-C (blue lines) is the farthest to the UL. Left Y-axis represents the half of current inter-electrode spacing (AB/2 or AO) at normal scale





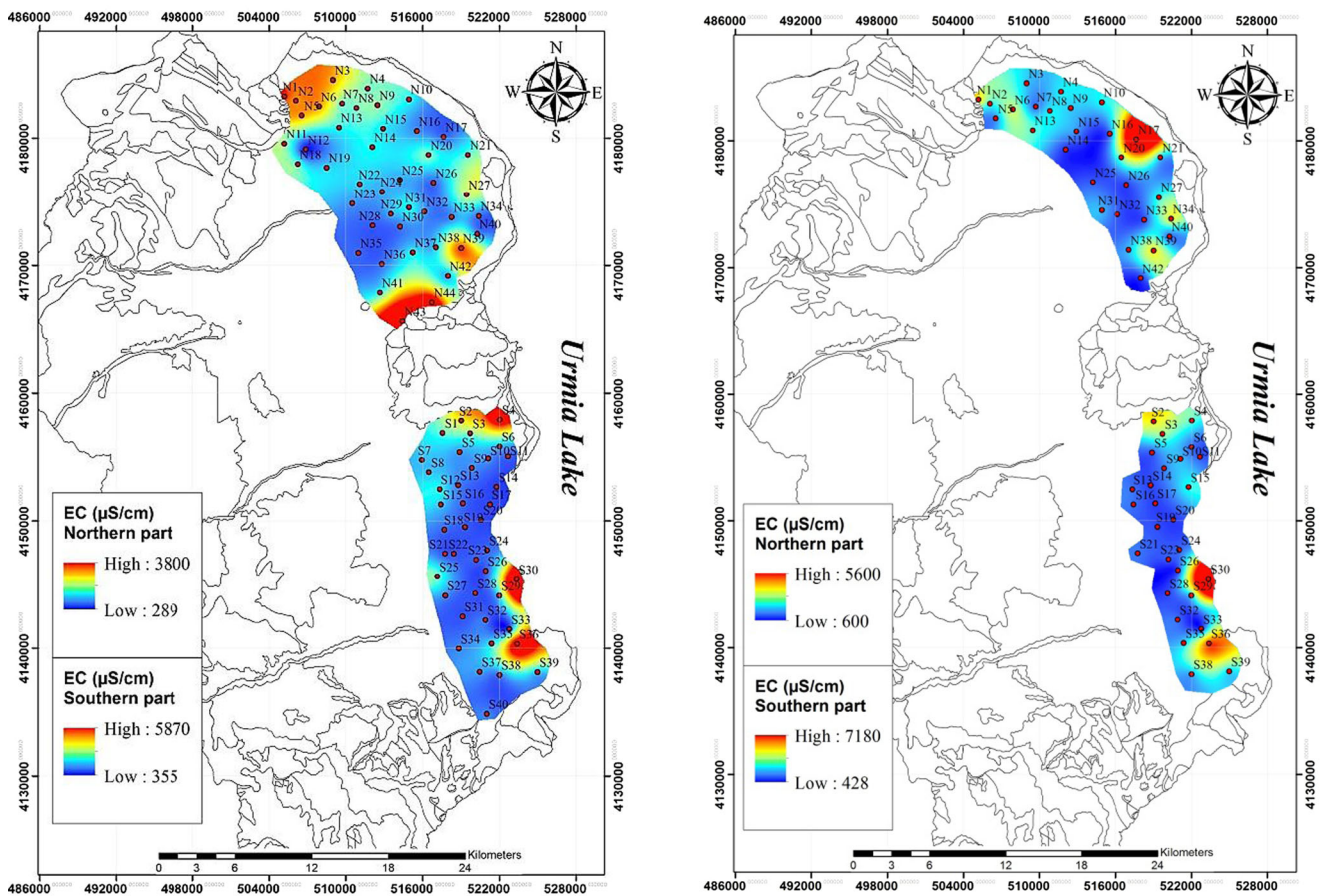


**Fig. 6** The EC values of groundwater samples in July 2014 (left) and September 2014 (right)

Boron is typically adsorbed during sea/saltwater intrusion (Jones et al. 1999). Boron tends to be adsorbed onto clay minerals and oxides, particularly under high salinity conditions. Consequently, saline groundwater associated with sea/saltwater intrusion is characterized by low B/Cl ratio relative to those of saline water body (Vengosh et al. 1994; Vengosh 1998; Vengosh et al. 1999a, b; Vengosh 2014).

Desorption is promoted by a decrease in ionic strength (Goldberg et al. 1993), so it would accompany the displacement of saline/saltwater from an aquifer by freshwater. The water chemistry data for three wet and dry periods show that, in areas affected by freshwater flushing, the concentration of B in the wet seasons is greater than it in the dry season (see the distribution of samples in Fig. 7). The concentration of B in June 2014, September 2014, and May 2015 changed between 0.3–64, 0.8–25.6, and 0.3–6.2 ppm, respectively. Note that the lower concentration of B in May 2015 is because of the small number of samples in this period. In other words, some freshwaters with possible high B contents were not sampled.

As shown in Fig. 7, high-boron contents have been detected, not only near the shoreline, where probably UL saltwater intrusion occurs, but also in the inland part of the aquifer. In addition, in the collected samples from UL, B/Cl ratios in the wet seasons are higher than the dry season (Fig. 7). The mean values of boron in UL in June 2014 and May 2015 are 420 and 1020 mg/l, respectively, while for the dry season it is equal to 46.1 mg/l. Therefore, by considering the significant decrease in B concentration and increase of Cl<sup>-</sup> in UL in the dry season, it can be concluded that by ending the precipitation and decreasing surface and possibly groundwater inflows to the UL which result in its salinity increase, the main cause for boron decrease is probably adsorption by clay minerals in the area. The intrusion of saline/saltwater into coastal aquifers is also associated with redox conditions along the saltwater-freshwater interface. In addition, saline groundwater associated with saline/saltwater intrusion is characterized by low SO<sub>4</sub><sup>2-</sup>/Cl<sup>-</sup> ratios (<0.05) (Krouse and Mayer 2000). The assessment of groundwater chemistry in the coastal area of UA indicates that

**Table 3** Ranges of B/Cl and Br/Cl ratios for selected sources of Cl, B, and Br in groundwater

Source	B (mg/l)	Br (mg/l)	Cl (mg/l)	B/Cl		Br/Cl		Reference
				Mass ratio ( $\times 10^{-3}$ )	Molar ratio ( $\times 10^{-3}$ )	Mass ratio ( $\times 10^{-3}$ )	Molar ratio ( $\times 10^{-3}$ )	
Sea/salt water intrusion								
Djeffara aquifer, Tunisia	–	84	22,160	–	–	3.97	1.68	Trabelsi et al. (2012)
Coastal aquifer, Israel	0.95	21.3	6304	0.15	0.49	3.38	1.5	Vengosh et al. (1994)
Salinas Valley, California	0.24	5.4	1670	0.15	0.48	3.23	1.44	Vengosh et al. (2002)
Urmia Aquifer, Iran	0.03–64	0.1–9.65	6.1–2061.4	0.66–740.74	2.16–2429.16	0.72–723.46	0.32–276.62	Present study
Saline lakes								
Salton Sea								
	12	13	17,000	0.71	2.31	0.76	0.34	Schroeder and Rivera (1993)
Dead Sea	59.69	4500	224,200	0.24	0.8	20.07	8.91	Starinsky (1974)
Great Salt Lake	13.32	50.9	147,000	0.09	0.29	0.34	0.15	Jones et al. (2009), Jones and Deocampo (2003)
Urmia Lake, Iran	46.1–1020	5.94–9.52	160,964–252687.2	0.18–6.34	0.60–20.78	0.036–0.038	0.016–0.017	Present study
Saline plumes and upcoming of brines								
Michigan basin brines, USA								
	–	315–4210	75,800–251,000	–	–	4.15–16.77	1.84–7.45	Wilson and Long (1993)
Coastal aquifer, Israel (Beer Toviyya)	0.50	3.5	1125	0.45	1.48	3.11	1.38	Vengosh et al. (1999a, b)
Ogallala aquifer, Texas	–	6.2	36,120	–	–	0.17	0.08	Mehta et al. (2000a, b)
Dammam aquifer, Kuwait	1.5	–	1241	1.21	3.96	–	–	Al-Ruwaih (1995)
Jordan Vally, Jericho, Cenomanian aquifer	–	83	4950	–	–	16.77	7.44	Marie and Vengosh (2001)
Agricultural drainage								
Mendota, San Joaquin Valley, California								
	–	3.4	1210	–	–	2.81	1.25	Kharaka et al. (1996)
Imperial Valley, California	1.7	2.3	2600	0.65	2.14	0.88	0.39	Schroeder and Rivera (1993)
Volcanic contribution of halides								
–	–	–	500–1000	–	–	2.05–3.01	0.91–1.33	Alcala and Custodio (2008)
Sewage or septic tank effluent								
Septic tank effluent-median of 9 samples								
	–	0.05	35	–	–	1.4	6.4	Katz et al. (2010)
Dan Reclamation Project, Israel	0.5	0.4	361	1.39	4.54	1.11	0.49	Vengosh and Keren (1996)
Orleans, CapeCod, Massachusetts	0.2	–	950	0.21	0.69	–	–	De Simone et al. (1997)

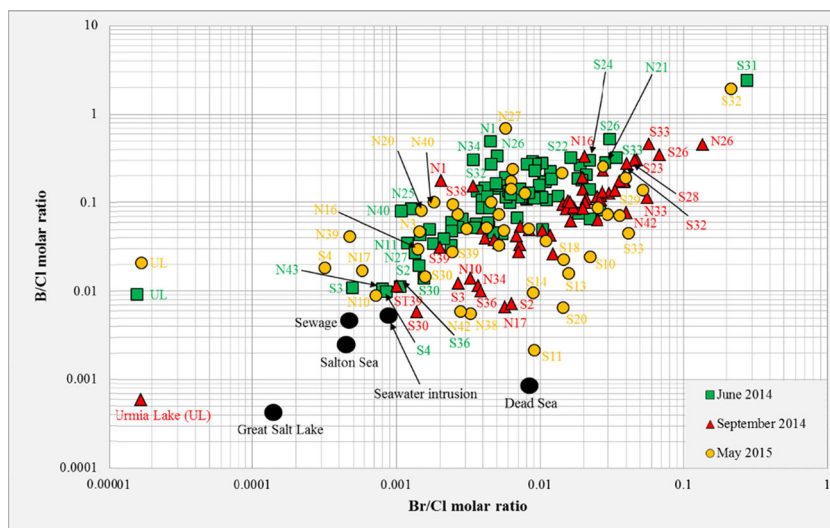
almost all the samples have higher  $\text{SO}_4^{2-}/\text{Cl}^-$  ratios than the reported value by Krouse and Mayer (2000) (<0.05) and UL (0.018, 0.22, and 0.44 in June 2014, September 2014, and May 2015, respectively). The average values of  $\text{SO}_4^{2-}/\text{Cl}^-$  ratio in groundwater samples are 3.02, 2.31, and 2.32 in June 2014, September 2014, and May 2015, respectively.

Saline  $\text{Na-HCO}_3$  water is often associated with high boron contents and B/Cl ratios (i.e., greater than seawater) as demonstrated in southern Mediterranean coastal aquifers (Vengosh et al. 2005), the Saloum delta aquifer of Senegal (Faye et al. 2005), sandstone and shale

aquifers in Michigan (Ravenscroft and McArthur, 2004), the delta aquifer of the Bengal Basin in southern Bangladesh (Ravenscroft and McArthur 2004; Halim et al. 2010), and the coastal aquifer of North Carolina (Vinson 2011).

The partial enrichment of boron relative to the expected conservative mixing between saline/saltwater and freshwater suggests that boron is mobilized from the adsorption sites (see Fig. 7). One possible explanation for the relative boron enrichment is that the equilibrium between adsorbed and dissolved boron is re-equilibrated during freshening processes resulting in desorption of boron. As shown in Fig. 7, some areas of UA

**Fig. 7** Plot of B/Cl vs. Br/Cl ratios in collected groundwater samples in the UA for three periods. Also shown are the B/Cl vs. Br/Cl ratios in sewage effluent (Vengosh and Keren 1996), seawater (Vengosh et al. 1994; Vengosh et al. 2002), saline lakes including Salton Sea (Schroeder and Rivera 1993), Dead Sea (Starinsky 1974), and Great Salt Lake (Jones and Deocampo 2003; Jones et al. 2009)



show evidence of saltwater intrusion (low Na/Cl and B/Cl ratios) while others show evidence of freshening (high Na/Cl and B/Cl ratios). The relatively strong correlation ( $R^2=0.74$ ) between Na/Cl and B/Cl ratios for the dry season (September 2014) that characterizes many of the saline Na–HCO<sub>3</sub> type groundwaters proposes that the influx of low-saline, Ca<sup>2+</sup>-rich, and low B concentration waters to the saline sites triggers the B mobilization to the water which leads to increase in B concentration. In contrast, for the wet seasons (June 2014 and May 2015), there are weak correlations ( $R^2=0.26$  and  $R^2=0.25$ , respectively) between Na/Cl and B/Cl ratios, which indicates that the boron mobilization is more limited in the wet seasons.

As a result, boron is enriched in desalted water with obviously high B/Cl ratios (Prats et al. 2000; Sagiv and Semiat 2004; Parks and Edwards 2005; Geffen et al. 2006; Hyung and Kim, 2006; Georghiou and Pashafidis 2007; Cengeloglu et al. 2008; Kloppmann et al. 2008; Ozturk et al. 2008; Mane et al. 2009; Tu et al. 2011; Vinson 2011). The B/Cl of desalted water can reach 0.4 (Kloppmann et al. 2008). In this study, B/Cl ratio in Urmia groundwater samples reach as high as 0.3, compared to  $18 \times 10^{-5}$  in saltwater of UL, a 1666-fold enrichment.

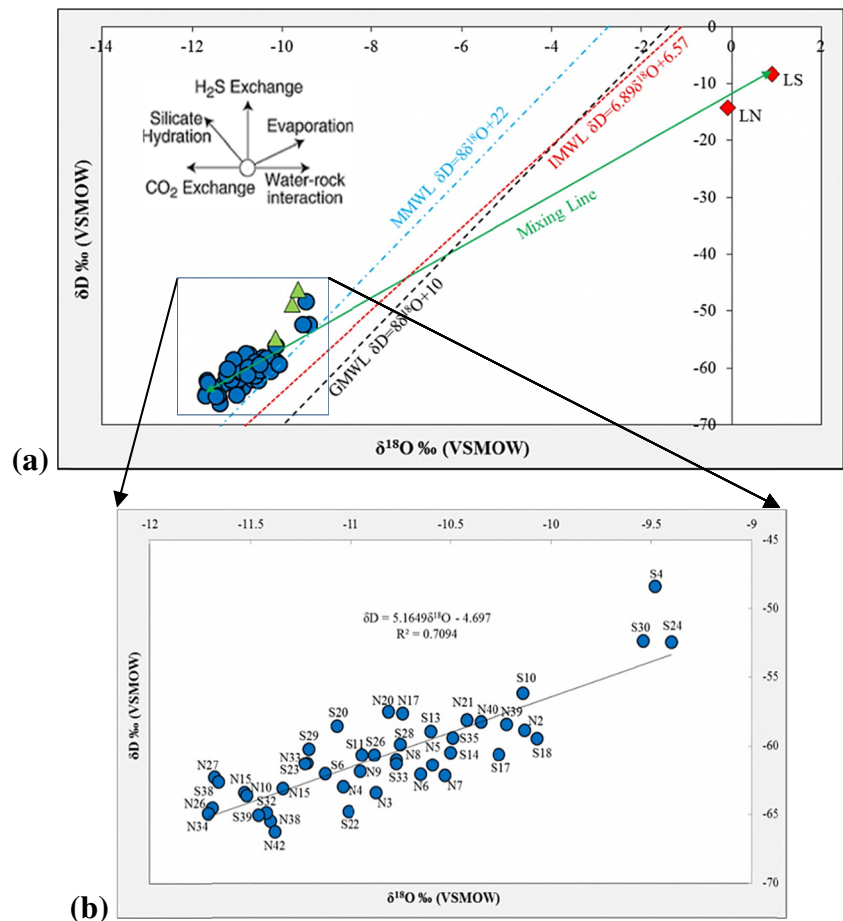
The most common tracers that have been extensively used for delineating salinity sources are halogen ratios, due to the basic assumption that halogens behave conservatively in aquifer systems. In particular, the bromide to chloride ratio has been used extensively to delineate salinization processes (Cartwright et al. 2004; Panno et al. 2006; Leybourne and Goodfellow 2007; Freeman 2007; Mandilaras et al. 2008; Cartwright et al. 2009; Katz et al. 2011; Warner et al. 2012). The nature and mechanism by which the saline waters originated (e.g., evaporation of sea/saltwater beyond halite saturation, dissolution of halite, domestic wastewater) will control

the Br/Cl ratios of the brine and consequently the bromide content of the salinized water.

While some salinity sources have distinctive low Br/Cl ratios (e.g., wastewater, deicing, evaporite dissolution) relative to other sources with high Br/Cl ratios (e.g., brines evolved from evaporated seawater, animal waste, coal ash), possible overlaps may occur. Furthermore, bromide may not always behave as a conservative tracer, as laboratory-controlled adsorption experiments have shown some bromide retention at pH < 7 can lead to modification of Br/Cl ratios during water transport in clay-rich systems (Goldberg and Kabengi 2010). According to the measured pH of groundwater samples in UA, 16 samples in June 2014, 1 sample in September 2014, and 1 sample in May 2015 show pH < 7. Note that almost in all these 18 samples, the pH values are very close to 7. In addition to sorption on clay minerals in aquifer matrix, Br<sup>-</sup> concentration and consequently Br/Cl ratios can modify by decomposition of organic matters that can add Br<sup>-</sup> to freshwater, saline/saltwater encroached, and fluids derived from evaporite mineral dissolution. Based on Br/Cl ion ratios (Fig. 7), the increase of salinity in the some parts of UA may be attributed to the invasion of diluted saltwater, base-exchange reactions of water with sediments and rocks in the area, and probably dissolution of evaporite deposits in some areas. We suggest that elevated Br/Cl ratios of saline waters compared to UL saltwater may be explained by differential uptake of Br<sup>-</sup> and Cl<sup>-</sup> during groundwater evolution through water–soil/rock reaction.

The ability to distinguish direct saline/saltwater intrusion from mixing of saline groundwater originating from displacement of saline/saltwater and freshening could be important for predicting salinization processes. Direct saline/saltwater intrusion would result in accelerated salinization rates, while mixing with saline groundwater that originated from diluted saline/saltwater could induce much lower salinization rates.

**Fig. 8 a** The  $\delta^{18}\text{O}$  vs.  $\delta\text{D}$  diagram for the all water data set showing the groundwater-Urmia saltwater mixing line, GMWL, MMWL, and IMWL; **b** zoom of **a**, showing the best-fit regression line for collected groundwater samples (circles: groundwater; diamonds: UL water (LN: northern part, LS: southern part); triangles: perennial rivers). In **b**, the river samples are not plotted



In some cases, the Br/Cl and B/Cl ratios of groundwater samples decrease with increasing salinity, which suggests that the major possible mechanisms of salinization of the those groundwater samples in the UA are mixing with saline groundwater that originated from diluted saline/saltwater, base-exchange reactions, and dissolution of salts stored in the unsaturated zone (Warner et al. 2010, 2013).

Based on our analysis of the data mentioned above and as shown in Table 3, other sources of salinization can be taken into account to change the concentration of  $\text{Cl}^-$ ,  $\text{Br}^-$ , and B, as well as the mass or molar ratios. Thus, comprehensive studies are needed to determine the role of these sources on water chemistry. It should be noted that, in this study, in order to reduce the adverse effect on water chemistry, we tried to collect the samples from wells that are far from pollution sources such as sewage.

**Hydrogen and oxygen-stable isotopes** T2 type tracers include water isotopes ( $\delta^{18}\text{O}$  and  $\delta\text{D}$ ) and ion concentrations. These tracers are used to identify evaporation (increase of  $\delta^{18}\text{O}$  and  $\delta\text{D}$ ) and mixing with external groundwater (depends on composition of external groundwater can lead to increase, decrease, or remain unchanged the  $\delta^{18}\text{O}$  and  $\delta\text{D}$ ). These tracers cannot use to identify salt dissolution.

One of the common conservative tracers for salinization studies are the stable isotopes of the water molecule, oxygen ( $\delta^{18}\text{O}$ ) and hydrogen ( $\delta\text{D}$ ) isotopes. The use of stable isotopes of oxygen and hydrogen for tracing salinity sources in surface water may be complicated by evaporation effects that will result in enrichment of  $\delta^{18}\text{O}$  and  $\delta\text{D}$  combined with low  $\delta^{18}\text{O}/\delta\text{D}$  ratios relative to the original composition of the saline water. However, natural or artificial recharge of saline/salt surface water into an aquifer may be identified by distinctive enriched  $\delta^{18}\text{O}$  and  $\delta\text{D}$  compositions.

Figure 8a shows contrasting isotopes compositions of coastal groundwater samples versus UL saltwater in May 2015. In addition, the water-stable isotopic composition for three perennial rivers is presented. Groundwater samples have  $\delta\text{D}$  in the range from  $-66.26$  to  $-48.41$  ‰, while  $\delta^{18}\text{O}$  is between  $-11.71$  and  $-9.4$  ‰. In the northern (deep) and southern (shallow) parts of UL, the  $\delta\text{D}$  is equal to  $-14.25$  and  $-8.35$  ‰, and  $\delta^{18}\text{O}$  is equal to  $-0.09$  and  $0.89$  ‰, respectively.

In Fig. 8a, the groundwater data cluster a little higher the East Mediterranean Meteoric Water Line (MMWL; Gat and Carmi 1970),  $\delta\text{D} = 8\delta^{18}\text{O} + 22$ , and they significantly depart from the Global Meteoric Water Line (GMWL; Craig 1961),  $\delta\text{D} = 8\delta^{18}\text{O} + 10$ , and the Iranian Meteoric Water Line (IMWL; Shamsi and Kazemi 2014),  $\delta\text{D} = 6.89\delta^{18}\text{O} + 6.57$ .

The results confirm clearly that we could not absolutely say that the groundwater samples collected in the coastal area of UA show the local meteoric derivation (i.e., IMWL). As mentioned, this area resides on the eastern flank of the Zagros Mountains at the eastern extent of the Mediterranean-type climate, according to the Global Bioclimatic Classification System (Martinez et al. 1999). Moisture originated from Mediterranean Sea is transported by cyclonic disturbances. The NW-SE trending Zagros mountain belt creates a barrier to the eastward penetration of these cyclones, affecting the amount of precipitation that reaches the interior of Iran. Therefore, more distance of data cluster from GMWL than IMWL can be justified.

The slope of the fitting line of groundwater data (the black line in Fig. 8b) given as:  $\delta D = 5.16\delta^{18}O + 4.69$  and  $R^2 = 0.709$ , is significantly lower than the Global, Mediterranean, and Iranian meteoric water lines. A comparison of the locally infiltrating and movement of groundwater to the east (UL) has demonstrated negligible evaporative processes in the soil during infiltration. This is mainly because of low mean annual temperature (11.52 °C) and relatively high precipitation (346.3 mm) in the area. Such a low slope in the  $\delta^{18}O$ - $\delta D$  relationship may be therefore due to isotopic fractionations upon groundwater infiltration and underground circulation. This process is a result of arid or semi-arid climatic conditions characterizing an area that has also been observed by Zimmerman et al. (1967) and Leontiadis et al. (1996). We noticed that all groundwater samples are depleted with respect to  $\delta^{18}O$  (-11.71 to -9.4‰) and  $\delta D$  (-66.26 to -48.41‰), represented in Fig. 8b. These samples were found on the locations where the groundwater is generally fresh. In addition, most of saline samples with more positive isotopic values were observed in the marginal (next to UL) areas.

The results of stable isotopes (Fig. 8) and B/Cl vs. Br/Cl ratios (Fig. 7) show that some saline samples (low B/Cl and Br/Cl ratios) are depleted with respect to  $\delta^{18}O$  and  $\delta D$ . As mentioned, stable isotopes of hydrogen and oxygen cannot

be used to identify salt dissolution. In this case, due to freshwaters flushing, the wells that are excavated at the coastal playas and salty sediments could have more depleted isotopes, more  $Cl^-$ , and consequently smaller B/Cl and Br/Cl ratios.

Such mixing relations on the continent are further manifested by the  $\delta^{18}O$  vs.  $Cl^-$  plot presented in Fig. 9. As shown, almost all groundwater samples show the small increase in  $\delta^{18}O$  values mainly from -9.4 to -11.71‰, while the  $Cl^-$  values differ from 6.87 to 1320 mg/l. The two samples with largest  $\delta^{18}O$  and  $Cl^-$  contents (shown as red diamonds in Fig. 9) represent the UL end-member. The  $Cl^-$  percentage of UL is represented on the mixing line. Distribution of samples on  $\delta^{18}O$  vs.  $Cl^-$  diagram (Fig. 9) indicates that all the samples have the  $Cl^-$  concentration less than 0.1 % of UL  $Cl^-$  content. Based on Fig. 9, just three samples include S30, S4, and S24 have  $\delta^{18}O$  values greater than -10‰, so this may be attributed to more evaporation in these sites than other sampling points. Using the values of  $\delta^{18}O$  vs.  $Cl^-$  can help us to determine the potential impacts of evaporite dissolution on samples, despite the fact that water-stable isotopes are not applicable for this case. Some samples (e.g., S24), which are relatively enriched with respect to  $\delta^{18}O$  and  $\delta D$  (Fig. 8), have the small  $Cl^-$  concentration. This means that some processes such as long residence time at the time of sampling and probably high groundwater level in the wells (and consequently more evaporation and isotopic enrichment) can be considered as effective factors for this phenomenon. In this area, S30 is the saltiest sample (EC values between 5870 and 7180  $\mu S/cm$  in wet and dry seasons, respectively).

The deuterium excess “d-excess”, defined by Dansgaard (1964) as  $d = \delta D - 8\delta^{18}O$ , allows further insight into the evolution of groundwater salinity to be gained. For the GMWL of Craig (1961), the d-excess is 10‰. Figure 10 displays the relationship between  $\delta^{18}O$  and the d-excess (generally varying between 21.11 and 31.16‰) in the Urmia groundwater samples. The d-excess values for northern and southern parts of UL are -13.53 and -15.47‰, respectively. In general,  $\delta^{18}O$

**Fig. 9** Relationship between chloride content and isotopic signature of water samples as a means to main possible differentiate hydrogeological processes in the area. The  $Cl^-$  percentage of UL is represented on the mixing line. The symbols are as in Fig. 8

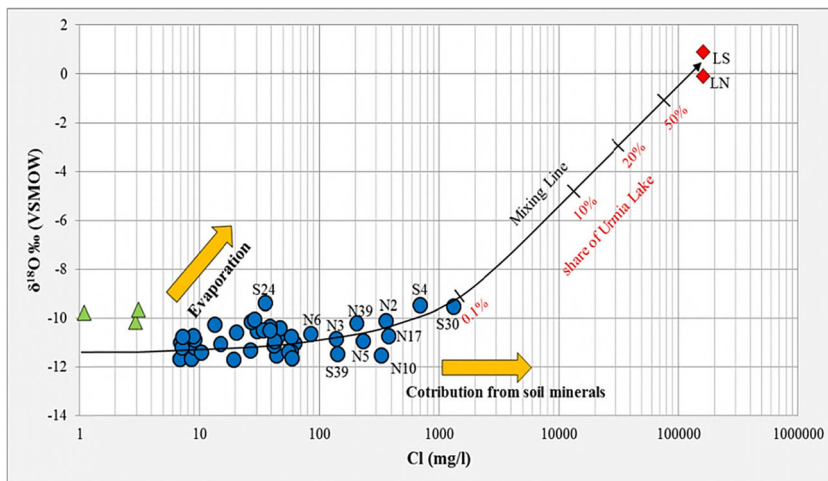
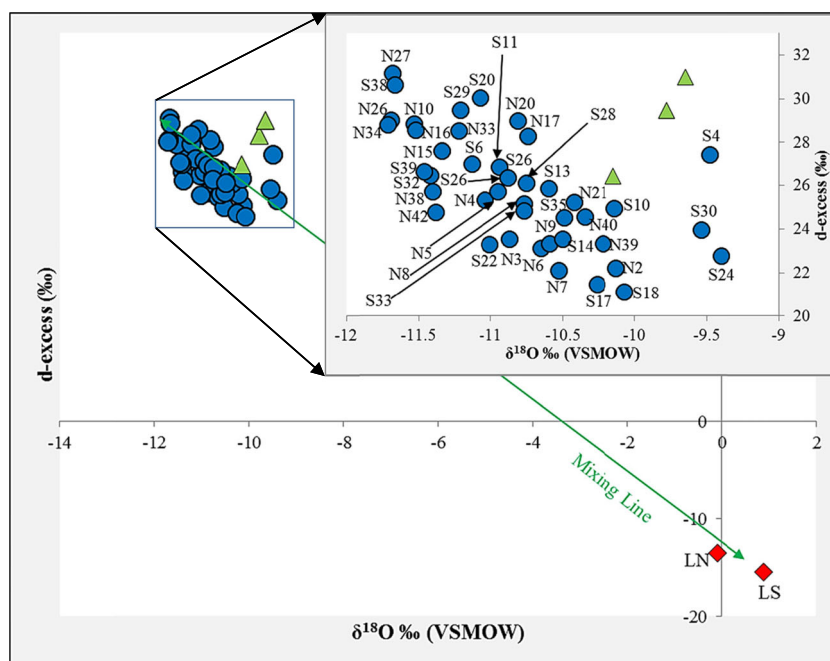


**Fig. 10** Plot of d-excess vs.  $\delta^{18}\text{O}$  for water samples. The symbols are as in Fig. 8



was negatively correlated with the d-excess (Fig. 10). The d-excess value is another index of the evaporation effect on the physicochemical characteristics of water: that is, if the water evaporates, the d-excess generally decreases (Han et al. 2011). The d-excess values lower than 10‰ (Han et al. 2009) and around 5‰ (Carol et al. 2009) suggest the isotopic composition in groundwater samples is characteristic of semi-arid climate. It means that groundwater has undergone evaporation prior to infiltration. As shown, the minimum d-excess value in Urmia groundwater samples is 21.11‰. Generally, lower values of  $\delta\text{D}$  and  $\delta^{18}\text{O}$  indicate a colder climatic signal during recharge.

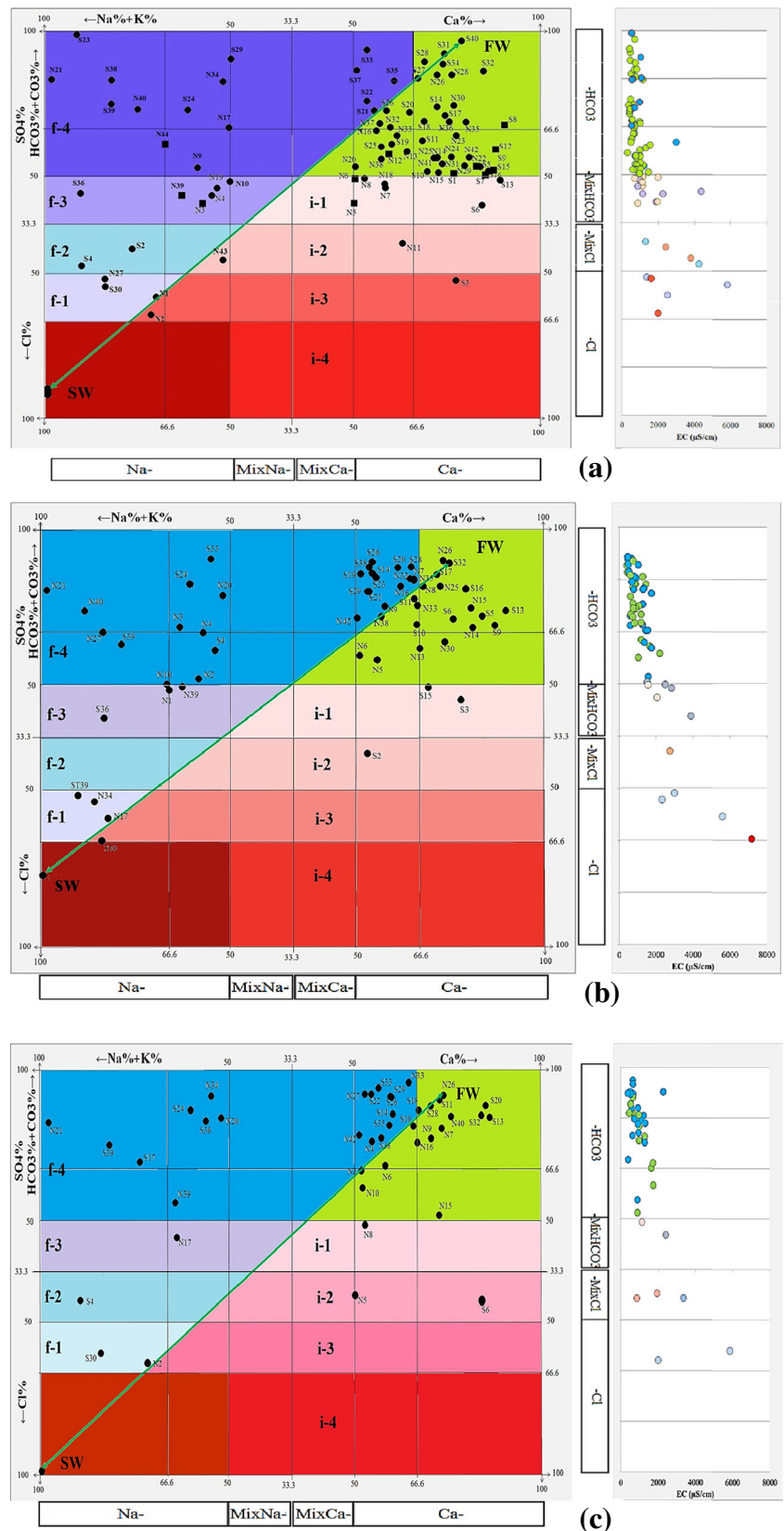
It should be noted that while the d-excess of all water samples are high, some groundwater samples show even higher values than surface water. Since surface water is directly evaporated, the high d-excess in some groundwaters most likely arises from relatively rapid incorporation of recycled precipitation (Marfia et al. 2004). The d-excess values propose the following: incoming vapors from UL are mixed with an evaporated moisture flux from the Urmia mainland and incoming vapors from the west (i.e., Mediterranean Sea), resulting in high d-excess in the surface and groundwaters. Based on Figs. 9 and 10, some samples with higher  $\delta^{18}\text{O}$  (e.g., S30, S4, and S24) are relatively correlated with evaporation process. Therefore, the d-excess is impacted by the influence of evaporation of the groundwater or infiltrating surface water (Han et al. 2011).

**Major ionic components of water** As mentioned in Sec. 3.2.2.1, T2 type tracers include water isotopes and ion concentrations. The Hydrochemical Facies Evolution Diagram

(HFE-D) (proposed by Giménez-Forcada et al. 2010) provides an easy way to identify the state of a coastal aquifer with respect to intrusion/freshening phases that takes place over time and which are identified by the distribution of anion and cation percentages in the square diagram.

In the HFE-Diagram (Fig. 11), four main facies are recognized: Na–Cl, sea/saltwater, Ca– $\text{HCO}_3$ , natural freshwater, Ca–Cl, salinized water with reverse cation-exchange, and Na– $\text{HCO}_3$ , salinized water with direct cation exchange. These four facies make up the processes. The hydrochemical facies types located above and to the left of the conservative mixing line are representative of freshening, but facies types situated below and to the right of the conservative mixing line characterize the sea/saltwater intrusion phase. Facies types located in the center of HFE-diagram can be considered as a member of either the freshening or intrusion phases, but this be determined by their location compared to the theoretical mixing line and, therefore, on the chemical composition of freshwater. The freshwater composition selected corresponds to a theoretical freshwater that takes account of the set of waters represented. For a set of groundwater samples, the highest percentages of cation (maximum value of  $\text{Ca}^{2+}$  (or  $\text{Mg}^{2+}$ )) and anion (maximum value of  $\text{HCO}_3^-$  (or  $\text{SO}_4^{2-}$ )) in freshwater are chosen. The highest percentages of  $\text{Ca}^{2+}$  and  $\text{HCO}_3^-$  do not have to relate to the same water sample, and so it is called the theoretical freshwater (it may or may not really exist). The reason for this is to guarantee that all the water samples are represented by one of the two fields that differentiates the conservative mixing line in the HFE-Diagram and

**Fig. 11** Representation of collected water samples in **a** June 2014, **b** September 2014, and **c** May 2015 on the HFE-Diagram (*square symbol* indicates that  $\text{SO}_4^{2-}$  value in sample is higher than other anions). *On the right*, the groundwater samples have been represented in terms of their EC values



which corresponds to the intrusion and freshening phases.

In the intrusion and freshening fields, various sub-steps can be identified, following the salinity evolution through the  $\text{Cl}^-$



percentage. The freshening sub-steps are including f-1, f-2, f-3, f-4, and FW (representative freshwater composition). In this diagram, the intrusion sub-steps related to the sea/saltwater intrusion phase are represented as i-1, i-2, i-3, i-4, and SW (representative sea/saltwater composition).

When the aquifer is in the freshening phase (recharge process), it initiates from an initial state in which the aquifer is totally salinized by sea/saltwater intrusion: then, from inland towards the coast areas, the recharge (fresh) water begins to rinse the aquifer which is in balance with the Na–Cl (halite) facies. The first sub-step in the freshening process is the sub-step “f-1” that is characterized by the distal freshening facies MixNa-Cl. Gradually, the groundwater chemistry changes to sub-step “f-2” (MixNa-MixCl) and “f-3” (MixCa-MixHCO<sub>3</sub>, Ca-MixHCO<sub>3</sub>), and so to sub-step “f-4” characterized by the proximal freshening facies “f-4” (Ca-HCO<sub>3</sub>, %Ca < 66.6). Finally, the total recovery process (freshening) of the aquifer is recognized by the Ca–HCO<sub>3</sub> facies.

In the sea/saltwater intrusion phase, there is an initial moment when the aquifer is completely filled with “freshwater” (or Ca–HCO<sub>3</sub> facies), which gradually changes to the proximal intrusion facies MixNa-Cl. During intrusion process, the water evolves from sub-step “i-1”, characterized by the distal intrusion facies, Ca-MixHCO<sub>3</sub>, to sub-step “i-2” (MixCa-MixCl, Ca-MixCl), and then to sub-steps “i-3” (MixNa-Cl (50 < %Cl < 66.6), MixCa-Cl, Ca–Cl), and “i-4”, which is identified by the proximal intrusion facies MixNa-Cl (%Cl > 66.6)). Finally, in this phase, Na–Cl occupies the whole aquifer. All sub-steps of sea/saltwater intrusion phase are characterized by higher cation values than conservative mixing line, displaying the contribution of reverse cation-exchange reactions.

In Fig. 11, all collected groundwater samples during three sampling periods are represented in the HFE-D along with the conservative mixing line for UL saltwater and freshwater. The percentages of samples for each sub-step in freshening and intrusion stages for three sampling periods are presented in Table 4. As shown in Table 4, in June 2014, September 2014, and May 2015, 13.09, 5.26, and 7.14 % of samples are located in the intrusion field, respectively.

Distribution of samples on HFE-D for three wet and dry seasons indicates clearly that the recharge of the aquifer with Ca–HCO<sub>3</sub> groundwater seems sufficient for direct cation-exchange reactions to occur and reach the next facies in the Na–HCO<sub>3</sub> freshening phase. It should be noted that, in the dry season (September 2014), like the wet seasons (June 2014 and May 2015), increasing the groundwater exploitation leads to movement of freshwaters from recharge zones in the western mountains. In the UA, the main recharge areas are located: in the north, west, and south of the plain. Four perennial rivers which are inflowing from the west of this plain can be considered as other rechargers of the aquifer. Meanwhile, the UL is located in the east of UA.

On the other hand, the Urmia saltwater encroachment to the aquifer with characteristic –Cl facies waters seems insufficient for changing the water chemistry, increasing the Cl<sup>-</sup> content and reaching the Na-Cl facies in the intrusion phase. In the dry season, by increasing the water exploitation from the aquifer, additional saltwater intrusion is not found. The main reason may be the existence of fine-grained sediments in the coastal areas that act as a natural barrier. Table 4 lists the criteria for separating sub-steps for freshening and intrusion phases. On the right side of the HFE diagrams, the percentage of anions is correlated with the groundwater salinity, via the representation of EC in the X-axis. Generally, groundwater samples in

**Table 4** The criteria to assign the numerical values for each sub-step (Giménez-Forcada 2014) and distribution of sub-steps for freshening and intrusion phases for three periods

Sub-step	Anion facies	Ion percentage	Cation-exchange evaluation	June 2014 N (%)	September 2014 N (%)	May 2015 N (%)
Freshwater (FW)	–HCO <sub>3</sub>	HCO <sub>3</sub> <sup>-</sup> > 50 Ca <sup>2+</sup> > 66.6	-	62 (73.81)	47 (82.47)	35 (83.33)
f-4	–HCO <sub>3</sub>	HCO <sub>3</sub> <sup>-</sup> > 50	freshening phase,			
f-3	–MixHCO <sub>3</sub>	50 ≥ HCO <sub>3</sub> <sup>-</sup> > 33.3	X <sub>sample</sub> < X <sub>theoretical</sub> , direct cation-exchange	6 (7.15)	3 (5.26)	1 (2.38)
f-2	–MixCl	33.3 < Cl <sup>-</sup> ≤ 50		2 (2.38)	0 (0.00)	1 (2.38)
f-1	–Cl	50 < Cl <sup>-</sup> < 66.6		3 (3.57)	3 (5.26)	2 (4.76)
i-1	–MixHCO <sub>3</sub>	50 ≥ HCO <sub>3</sub> <sup>-</sup> > 33.3	X <sub>sample</sub> > X <sub>theoretical</sub> , reverse	7 (8.33)	2 (3.51)	1 (2.38)
i-2	–MixCl	33.3 < Cl <sup>-</sup> ≤ 50	cation-exchange	2 (2.38)	1 (1.75)	2 (4.76)
i-3	–Cl	50 < Cl <sup>-</sup> < 66.6		2 (2.38)	0 (0.00)	0 (0.00)
i-4	–Cl	Cl <sup>-</sup> > 66.6		0 (0.00)	1 (1.75)	0 (0.00)
Saltwater (SW)	–Cl	Cl <sup>-</sup> > 66.6 Na <sup>+</sup> > 50	-			

freshening phase have lower EC values than those corresponding to intrusion phase.

The results indicate that most groundwater samples collected from the same well during different periods show relatively similar behavior. The results demonstrate that the seasonal variability did not affect the characteristics of the groundwater; in this way, one can identify the main areas of recharge and the zones affected by salinization.

Note that, in some sampling points, the varying positions of the sub-steps on the three periods studied are a mark of the dynamism of the surface (UL)/groundwater bodies in UA, and it indicates what changes in water chemistry can be related to changes in the balance of the aquifer and the dynamics of the salinization from UL saltwater intrusion.

As stated before, almost certainly base-exchange reactions are the contributing factors in changing the water chemistry. In this study, base-exchange index (BEI) is calculated to determine the contribution of cation-exchange reactions in variations of groundwater chemistry. BEI can also be used to distinguish if an aquifer is undergoing salinization or freshening, or has been freshened or salinized in the past. According to Stuyfzand (2008), the best index (for a dolomite free aquifer system) is  $BEI = Na + K + Mg - 1.0716Cl$  (concentrations in meq/l). The factor 1.0716 is equal to  $[Na + K + Mg]/Cl$  (in meq/l) for mean ocean water (Riley and Skirrow 1975). For current investigation, the mean value of this factor for UL is equal to 1.7091. A positive BEI represents freshening due to cation-exchange, a negative BEI represents salinization because of reverse cation-exchange, and a BEI with a value of zero represents no cation-exchange. The classification of Stuyfzand is well known for its application in coastal areas for the determination of water types and the evaluation of geochemical processes (e.g., Vandenbohede et al. 2009; de Louw et al. 2010; Giménez-Forcada et al. 2010). The results show that most of the collected groundwater samples during three sampling periods have a positive value for BEI, indicating freshwater intrusion to the wells. The computed values of BEI show that just one sample (S3) in June 2014, three samples (S3, S30, and S36) in September 2014, and one sample (N10) in May 2015 are negative, indicating reverse cation-exchange and salinization of those samples.

In addition to BEI results which clearly indicate freshening mechanism as the dominant process in this area, saturation index (SI) calculations showed that all groundwater samples collected in these periods have negative saturation indices, which indicate undersaturation ( $SI < 0.5$ ) with respect to anhydrite ( $CaSO_4$ ), gypsum ( $CaSO_4 \cdot 2H_2O$ ), and halite ( $NaCl$ ), demonstrating the eventual dissolution of these minerals. Also, except in some cases (e.g., S30 and N40 saturated with respect to dolomite ( $CaMg(CO_3)_2$ ) and N39 saturated with respect to aragonite ( $CaCO_3$ ) and calcite ( $CaCO_3$ )), all other samples showed the undersaturation with respect to the carbonate minerals such as aragonite, calcite, and dolomite.

Therefore, the mentioned minerals are susceptible to dissolution. In the dry season (September 2014), the SI calculations show the more positive values with respect to dolomite, especially in the northern part of UA that indicate the higher potential for precipitation and deposition of dolomite in these sites. In hypersaline environments, precipitation is commonly rapid, and together with the high concentrations of foreign ions, it is difficult for dolomite to form because the precise Ca–Mg ordering required. Thus, dolomite probably forms most readily by a reduction in salinity, particularly in a schizohaline environment (alternating between hypersaline and near-fresh conditions, as in a phreatic mixing zone). Flushing saltwaters with freshwater lowers salinity but maintains a high Mg/Ca ratio; the interfering effect of foreign ions is reduced (Folk and Land 1975).

### The fresh/saltwater interface (the “zone of dispersion”)

We used the Ghyben-Herzberg relation (Bear 1979) to estimate the boundary between fresh and saline waters at the Urmia site. The equation relates the elevation of the water table to the elevation of the boundary of the interface between the freshwater and underlying saltwater zones of an aquifer and is based on the balance of the height of two columns of fluids of differing density (Reilly and Goodman 1985). The vertical profile of the fresh/saltwater interface normal to the shoreline tends to occur as a concave-upward wedge of freshwater bounded by saline/saltwater. This simplistic model ignores convection, dispersion, and diffusion phenomena frequently observed in coastal unconfined aquifers. It assumes that freshwater and seawater forms a sharp static contact (in reality it is in a dynamic equilibrium); the height of which,  $Z$ , is given as:

$$Z = \frac{\rho_f}{\rho_s - \rho_f} h \tag{1}$$

where  $h$  is the height of the groundwater table above the mean sea level, and  $\rho_f$  and  $\rho_s$  is the density of freshwater and seawater, respectively. Based on the difference between the density of freshwater ( $1.000 \text{ g/cm}^3$ ) and seawater ( $1.025 \text{ g/cm}^3$ ) at  $20^\circ \text{C}$ ,  $Z = 40 h$ .

The density of UL saltwater changed between  $1.27$  and  $1.30 \text{ g/cm}^3$  in wet and dry seasons (June 2014, September 2014, and May 2015). In this study, the value of  $1.27 \text{ g/cm}^3$  was considered for calculations of fresh/saltwater interface in the coastal areas of UA. According to the Ghyben-Herzberg approximation and density of  $1.27 \text{ g/cm}^3$  in UL, the depth of the transition zone in Urmia coastal line is about 3.7 times the groundwater elevation, compared to 40 times in aquifers next to the ocean. Based on density of water in UA and collected data from field surveys during June 2014–May 2015, we tried to provide the vertical profiles of fresh/saltwater interface in

six normal directions to the coastline. For this purpose, we used the water levels in target wells and of UL, depth of wells, water chemistry, water-stable isotopes, geophysical data, and sedimentological/stratigraphical results of previous studies.

The UL sediments are generally fine-grained, except at the conjunction of rivers to the Lake where coarser grains such sand and gravel are deposited. Sediments in the middle parts of the Lake mainly consist of fine clay to silt. A borehole with 180 m in depth which was drilled along Shahid Kalantary causeway (across the Lake with E-W direction) in 1992

indicates that the first sandy layer with thickness 2.5 m is located in depth 132 m and the second thin sandy layer is placed in depth 137 m. Observations in that year showed that the underground saline water overflowed from the borehole which was excavated to depth 137 m. The hydraulic pressure in that borehole was equal to 2.5 bars. In addition, sedimentary layers in depth 30–45 m had high resistance. Therefore, by considering the fine-grained sediments in the central parts of Lake and high hydraulic pressure in deep sediments, it can be concluded that there is no high hydraulic connection (i.e., free

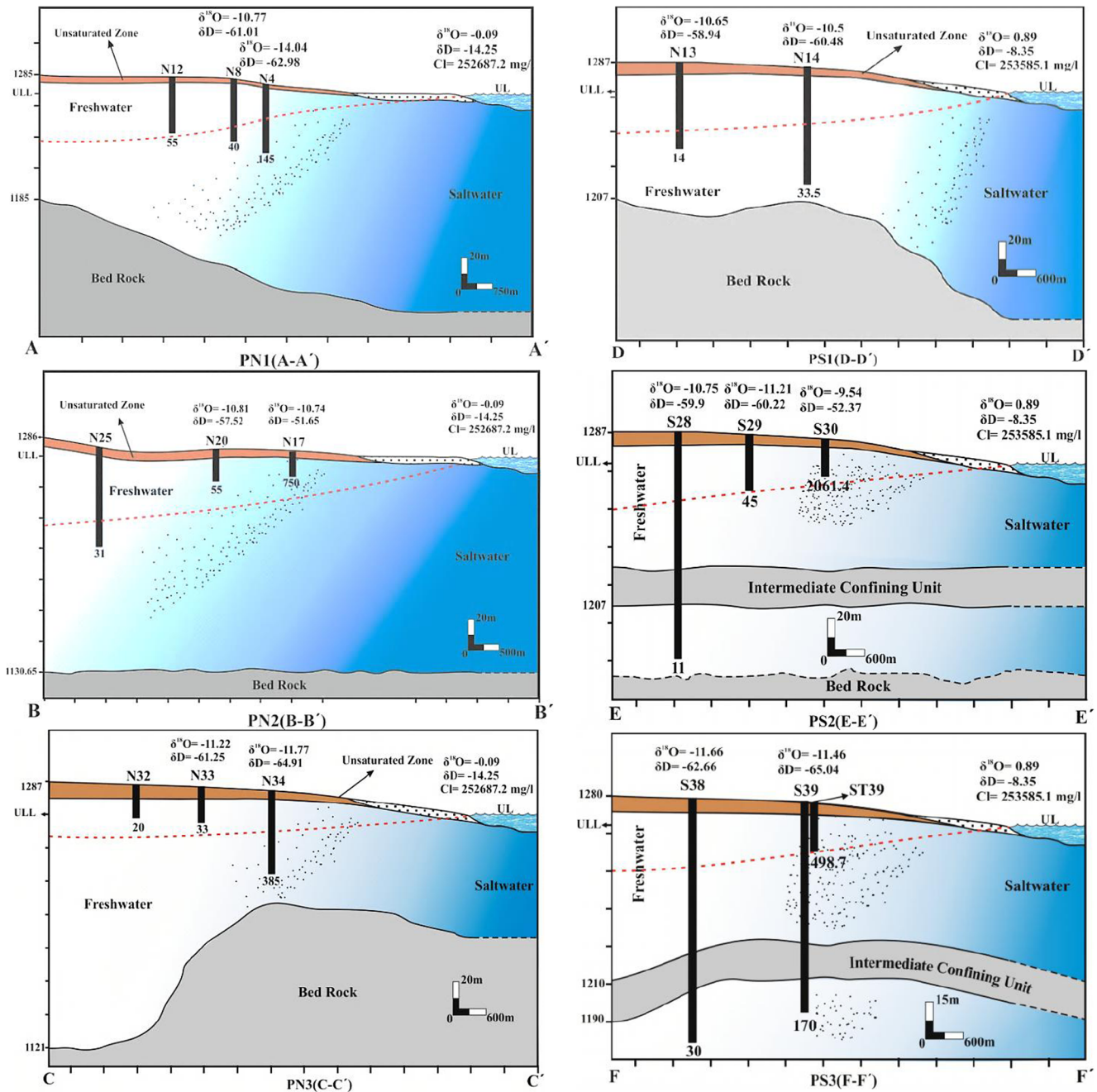


**Fig. 12** Generalized freshwater-saltwater profiles across the UA. Calculated depth of saltwater interface based on Ghyben-Herzberg law is presented in red dash. Chloride concentrations are displayed at the end of wells. Isotopic values are in per-mille (‰)

drainage) between Lake and beneath layers, but the sediments are fully saturated with recent and old saltwaters originated from UL. By considering the hard and thin salty layer in the UL floor and slower sedimentation rate for fine grains that lead to looseness of deposits in these areas, small and continuous leakage from the lake to underground sedimentary layers is occurring. Unconsolidated sediments in central and coastal parts of UL had thickness about 55 and 15 m, respectively.

The prepared salinity profiles based on hydrochemical data, geophysical sounding, and field observations are presented in Fig. 12. By considering more water density and less depth of UL than seas and oceans, and the main application of Ghyben-Herzberg law in seawater intrusion, the underground mixing of UL saltwater and groundwater in coastal UA is very complicated. Therefore, the Ghyben-Herzberg law could be discussed only as approximations (red dashes in Fig. 12). As shown, the  $\text{Cl}^-$  concentrations in the wells indicate that the front of salinity is reached just to the first wells in considered profiles. Only can be seen in profile PS2 (Fig. 12), the slightly enrichment of  $\delta\text{D}$  and  $\delta^{18}\text{O}$  values in near shoreline locations than inland wells. Therefore, the observed salinity in coastal areas (especially in sample S30) is due to the encroachment of highly diluted UL saltwater. Note that water chemistry in this area can be affected by other mentioned factors.

## Conclusions

The poor correlation between sampling depth and  $\text{Cl}^-$  concentrations indicated that the position of freshwater–saltwater interface is not uniformly distributed in the study area, and this was attributed to aquifer heterogeneities. In some samples, the Br/Cl and B/Cl ratios of groundwater samples decrease with increasing salinity, which suggests that the major mechanisms of salinization of those groundwater samples in the UA are base-exchange reactions between water and aquifer materials, mixing with saline groundwater that originated from diluted saline/saltwater, and maybe dissolution of salts stored in the unsaturated zone and salinization of the underlying shallow groundwater. Most of the collected groundwater samples during three sampling periods have a positive value for BEI, indicating freshwater intrusion to the wells. The computed values of BEI show that just one sample (S3) in June 2014, three samples (S3, S30, and S36) in September 2014, and one sample (N10) in May 2015 are negative, indicating reverse cation-exchange and salinization of groundwater samples. SI calculations showed that all groundwater samples collected in three sampling periods show negative saturation indices, which indicate undersaturation with respect to anhydrite, gypsum, and halite. Also, except in some cases (e.g., S30 and N40 saturated with respect to dolomite and N39 saturated with respect to aragonite and calcite), all other samples showed the undersaturation with respect to the carbonate minerals

such as aragonite, calcite, and dolomite. The hydrogeochemical characteristics based on BEI and SI show that changes in the chemical composition of groundwater are mainly controlled by the salinization process followed by cation-exchange reactions. Groundwater samples (wells) have  $\delta\text{D}$  in the range from  $-66.26$  to  $-48.41$  ‰, while  $\delta^{18}\text{O}$  is between  $-11.71$  and  $-9.4$  ‰. In the northern (deep) and southern (shallow) parts of UL, the  $\delta\text{D}$  is equal to  $-14.25$  and  $-8.35$  ‰, and also  $\delta^{18}\text{O}$  is equal to  $-0.09$  and  $0.89$  ‰, respectively. Almost all the groundwater samples are depleted with respect to the heavy isotope ( $\delta^{18}\text{O}$  between  $-11.71$  and  $-9.4$  ‰) that was found on the locations where the groundwater has a short residence time (freshwater). Most of samples with more positive values were observed in the marginal (close to shoreline) areas. Results of stable isotopes and B/Cl vs. Br/Cl diagram show that some saline samples (low B/Cl and Br/Cl ratios) are depleted with respect to  $\delta^{18}\text{O}$  and  $\delta\text{D}$ . As mentioned, stable isotopes of hydrogen and oxygen tracers cannot use to identify salt dissolution. In this case, due to freshwater flushing, the wells that are excavated at the coastal playas and salty sediments could had more depleted isotopes, more  $\text{Cl}^-$ , and consequently smaller B/Cl and Br/Cl ratios. The results of HFE diagram showed that because of the existence of salty and fine-grained sediments in the coastal areas that act as a natural barrier increasing the groundwater exploitation leads to movement of freshwaters from recharge zones in the western mountains not saltwater from UL. In some areas, particularly in the southern part, there is no sign of seasonal variation in groundwater quality. The highly permeable sediments at the junction of the river to UL at the east coastal aquifer are characterized by low hydraulic gradient and high hydraulic conductivity. These properties enhance the salinization of groundwater observed in the study area. The main factors influencing the salinity are base-exchange reactions, invasion of highly diluted saltwater, dissolution of salty sediments, and water chemistry evolution along flow paths.

**Acknowledgments** This is a part of Ph.D. dissertation of the senior author (V. Amiri), and he would like to thank the Geological Survey of Iran (GSI) for the financial support. The authors would like to thank Dr. Matthew Currell and another anonymous reviewer for their insightful comments. The first author would like to thank Mr. Ebrahim Naderi for his efficient help for drawing freshwater–saltwater profiles.

## References

- Alcala FJ, Custodio E (2008) Using the Cl/Br ratio as a tracer to identify the origin of salinity in aquifers in Spain and Portugal. *J Hydrol* 359: 189–207
- Al-Ruwaih FM (1995) Chemistry of groundwater in the Dammam Aquifer, Kuwait. *Hydrogeol J* 3:42–55

- Amiri V, Sohrabi N, Altafi Dadgar M (2015) Evaluation of groundwater chemistry and its suitability for drinking and agricultural uses in the Lenjanat plain, central Iran. *Environ Earth Sci* 74:6163–6176
- Amrhein C, Duff MC, Casey WH, Westcot DW (1998) Emerging problems with uranium, vanadium, molybdenum, chromium, and boron. In: Dudley LM, Guitjens JC (eds) *Agroecosystems and the environment: sources, control, and remediation of potentially toxic, trace element oxyanions*. American Association for the Advancement of Science, Washington, DC
- APHA (1985) *Standard methods for the examination of water and wastewater*, 16th edn. American Public Health Association, Washington DC
- Asfahani J, Abou Zakhem B (2013) Geoelectrical and hydrochemical investigations for characterizing the salt water intrusion in the Khanasser Valley, Northern Syria. *Acta Geophys* 61(2):422–444
- Backstrom M, Nilsson U, Hakansson K, Allard B, Karlsson S (2003) Speciation of heavy metals in road runoff and roadside total deposition. *Water Air Soil Pollut* 147:343–366
- Backstrom M, Karlsson S, Backman L, Folkesson L, Lind B (2004) Mobilisation of heavy metals by deicing salts in a roadside environment. *Water Res* 38:720–732
- Badv K, Derizadeh M (2005) Wellhead protection area delineation using the analytic element method. *Water Air Soil Pollut* 161:39–54
- Barbecot F, Marlin C, Gibert E, Dever L (2000) Hydrochemical and isotopic characterisation of the Bathonian and Bajocian coastal aquifer of the Caen area (northern France). *Appl Geochem* 15:791–805
- Bear J (1979) *Hydraulics of groundwater*. McGraw-Hill, New York, p 576
- Carol E, Kruse E, Mas-Pla J (2009) Hydrochemical and isotopic evidence of ground water salinization processes on the coastal plain of Samborombón Bay, Argentina. *J Hydrol* 365:335–345
- Cartwright I, Weaver TR, Fulton S, Nichol C, Reid M, Cheng X (2004) Hydrogeochemical and isotopic constraints on the origins of dryland salinity, Murray Basin, Victoria, Australia. *Appl Geochem* 19:1233–1254
- Cartwright I, Hall S, Tweed S, Leblanc M (2009) Geochemical and isotopic constraints on the interaction between saline lakes and groundwater in southeast Australia. *Hydrogeol J* 17:1991–2004
- Cengeloglu Y, Arslan G, Tor A, Kocak I, Dursun N (2008) Removal of boron from water by using reverse osmosis. *Sep Purif Technol* 64:141–146
- Craig H (1961) Isotopic variation in meteoric waters. *Science* 133:1702–1703
- Dansgaard W (1964) Stable isotopes in precipitation. *Tellus* 16:436–438
- Darling WG, Edmunds WM, Smedley PL (1997) Isotopic evidence for paleowaters in the British Isles. *Appl Geochem* 12:813–829
- de Louw PGB, Oude Essink GHP, Stuyfzand PJ, van der Zee Seatm (2010) Upward groundwater flow in boils as the dominant mechanism of salinization in deep polders, The Netherlands. *J Hydrol* 394:494–506
- De Simone LA, Howes BL, Barlow PM (1997) Mass-balance analysis of reactive transport and cation-exchange in a plume of wastewater-contaminated groundwater. *J Hydrol* 203:228–249
- Dregne HE (2002) Land degradation in the drylands. *Arid Land Res Manag* 16:99–132
- Duque C, Calvache ML, Pedrera A, Martin-Rosales W, Lopez-Chicano M (2008) Combined time domain electromagnetic soundings and gravimetry to determine marine intrusion in a detrital coastal aquifer (Southern Spain). *J Hydrol* 349:536–547
- Faye S, Maloszewski P, Stichler W, Trimborn P, Faye SC, Gaye CB (2005) Groundwater salinization in the Saloum (Senegal) delta aquifer: minor elements and isotopic indicators. *Sci Total Environ* 343:243–259
- Fidelibus MD, Calò G, Tinelli R, Tulipano L (2011) Salt ground waters in the Salento karstic coastal aquifer (Apulia, Southern Italy). In: Lambrakis N, Stournaras G, Katsanou K (eds) *Advances in the research of aquatic environment, environmental/earth sciences series*, vol 1. Springer, Berlin, pp 407–415
- Folk RL, Land LS (1975) Mg/Ca ratio and salinity: two controls over crystallization of dolomite. *AAPG Bull* 59(1):60–68
- Freeman JT (2007) The use of bromide and chloride mass ratios to differentiate salt-dissolution and formation brines in shallow groundwaters of the Western Canadian Sedimentary Basin. *Hydrogeol J* 15:1377–1385
- Gardner PM, Kirby SM (2011) Hydrogeologic and geochemical characterization of groundwater resources in Rush Valley, Tooele County, Utah. U.S. Geological Survey Scientific Investigations Report 2011-5068, 68p
- Gat JR, Carmi H (1970) Evolution of the isotopic composition of atmospheric waters in the Mediterranean Sea area. *J Geophys Res* 75:3039–3040
- Gaye CB (2001) Isotope techniques for monitoring groundwater salinization. *First International Conference on Saltwater Intrusion and Coastal Aquifers-Monitoring, Modeling, and Management*. Essaouira
- Geffen N, Semiat R, Eisen MS, Balazs Y, Katz I, Dosoretz CG (2006) Boron removal from water by complexation to polyol compounds. *J Membr Sci* 286:45–51
- Georghiou G, Pashafidis L (2007) Boron in groundwaters of Nicosia (Cyprus) and its treatment by reverse osmosis. *Desalination* 215:104–110
- Giménez-Forcada E (2014) Space/time development of seawater intrusion: a study case in Vinaroz coastal plain (Eastern Spain) using HFE-Diagram, and spatial distribution of hydrochemical facies. *J Hydrol* 517:617–627
- Giménez-Forcada E, Bencini A, Pranzini G (2010) Hydrogeochemical considerations about the origin of groundwater salinization in some coastal plains of Elba Island (Tuscany, Italy). *Environ Geochem Health* 32:243–257
- Goldberg S, Kabengi NJ (2010) Bromide adsorption by reference minerals and soils. *Vadose Zone J* 9:780–786
- Goldberg S, Forster HS, Heick EL (1993) Boron adsorption mechanisms on metal oxides, clay-minerals, and soils inferred from ionic-strength effects. *Soil Sci Soc Am* 57:704–708
- Goldberg S, Hyun S, Lee LS (2008) Chemical modeling of arsenic(III, V) and selenium(IV, VI) adsorption by soils surrounding ash disposal facilities. *Vadose Zone J* 7:1185–1192
- Gonfiantini R (1978) Standard for stable isotope measurements in natural compounds. *Nature* 271:534
- Halim MA, Majumder RK, Nessa SA, Hiroshiro Y, Sasaki K, Saha BB, Saepuloh A, Jinno K (2010) Evaluation of processes controlling the geochemical constituents in deep groundwater in Bangladesh: spatial variability on arsenic and boron enrichment. *J Hazard Mater* 180:50–62
- Han D, Liang X, Jin M, Currell MJ, Han Y, Song X (2009) Hydrogeochemical indicators of groundwater flow systems in the Yangwu River Alluvial Fan, Xinzhou Basin, Shanxi, China. *Environ Manag* 44:243–255
- Han D, Song X, Currell MJ, Cao G, Zhang Y, Kang Y (2011) A survey of groundwater levels and hydrogeochemistry in irrigated fields in the Karamay Agricultural Development Area, northwest China: implications for soil and groundwater salinity resulting from surface water transfer for irrigation. *J Hydrol* 405(3–4):217–234
- Hyung H, Kim J-H (2006) A mechanistic study on boron rejection by sea water reverse osmosis membranes. *J Membr Sci* 286:269–278
- ISO 5667-11 (1993) *Water quality. Sampling. Guidance on sampling of groundwaters*
- Jackson RB, Carpenter SR, Dahm CN, Mc Knight MDM, Naiman RJ, Postel SL, Running SW (2001) *Water in a changing world*. *Ecol Appl* 11:1027–1045
- Jalali M (2007) Salinization of groundwater in arid and semi-arid zones: an example Tajarak, western Iran. *Environ Geol* 52:1133–1149

- Jones BF, Deocampo DM (2003) Treatise on geochemistry, Volume 5. Editor: James I. Drever. Executive Editors: Heinrich D. Holland and Karl K. Turekian. pp. 605. ISBN 0-08-043751-6. Elsevier, pp.393-424
- Jones BF, Vengosh A, Rosenthal A, Yechieli Y (1999) Geochemical investigations. In: Bear J, Cheng AH-D, Sorek S, Ouazar D, Herrera H (eds) Seawater intrusion in coastal aquifers-concepts, methods, and practices. Kluwer Academic Publishers, Dordrecht, pp 51–69
- Jones BF, Naftz DL, Spencer RJ, Oviatt CG (2009) Geochemical evolution of Great Salt Lake, Utah, USA. *Aquat Geochem* 15:95–121
- Kamei T, Ikeda J, Ishida H, Ismda S, Onishi I, Partoazar H, Sasajima S, Nishimur S (1973) A general report on the geological and paleontological survey in Maragheh Area, North-West Iran. Internal Report, Geological Survey of Iran
- Katz BG, Griffin DW, McMahon PB, Harden H, Wade E, Hicks RW, Chanton J (2010) Fate of effluent-borne contaminants beneath septic tank drainfields overlying a karst aquifer. *J Environ Qual* 39: 1181–1195
- Katz BG, Eberts SM, Kauffman LJ (2011) Using Cl/Br ratios and other indicators to assess potential impacts on groundwater quality from septic systems: a review and examples from principal aquifers in the United States. *J Hydrol* 397:151–166
- Kharaka YK, Ambats G, Presser TS, Davis RA (1996) Removal of selenium from contaminated agricultural drainage water by nanofiltration membranes. *Appl Geochem* 11:797–802
- Khatami S (2013) Nonlinear chaotic and trend analyses of water level at Urmia Hypersaline Lake, Iran. M.Sc. Thesis report, TVVR 13/5012. Lund: Lund University
- Kloppmann W, Vengosh A, Guerrot C, Millot R, Pankratov I (2008) Isotope and ion selectivity in reverse osmosis desalination: geochemical tracers for man-made freshwater. *Environ Sci Technol* 42:4723–4731
- Koukadaki MA, Karatzas GP, Papadopoulou MP, Vafidis A (2007) Identification of the saline zone in a coastal aquifer using electrical tomography data and simulation. *Water Resour Manag* 21: 1881–1898
- Kouzana L, Benassi R, Ben mammou A, Sfar felfoul M (2010) Geophysical and hydrochemical study of the seawater intrusion in Mediterranean semi-arid zones. Case of the Korba coastal aquifer (Cap-Bon, Tunisia). *J Afr Earth Sci* 58:242–254
- Krouse HR, Mayer B (2000) Sulphur and oxygen isotopes in sulphate. In: Cook P, Herczeg AL (eds) Environmental tracers in subsurface hydrology. Kluwer, Boston, pp 195–231
- Leontiadis L, Vergis S, Christodoulou T (1996) Isotope hydrology study of areas in eastern Macedonia and Thrace, northern Greece. *J Hydrol* 182:1–17
- Leybourne MI, Goodfellow WD (2007) Br/Cl ratios and O, H, C, and B isotopic constraints on the origin of saline waters from eastern Canada. *Geochim Cosmochim Acta* 71:2209–2223
- Madani K (2014) Water management in Iran: what is causing the looming crisis? *J Environ Stud Sci* 4(4):315–328
- Mandilaras D, Lambrakis N, Stamatis G (2008) The role of bromide and iodide ions in the salinization mapping of the aquifer of Glafkos River basin (northwest Achaia, Greece). *Hydrol Process* 22: 611–622
- Mane PP, Park P-K, Hyung H, Brown JC, Kim J-H (2009) Modeling boron rejection in pilot- and full-scale reverse osmosis desalination processes. *J Membr Sci* 338:119–127
- Manning AH (2009) Ground-water temperature, noble gas, and carbon isotope data from the Española Basin, New Mexico. U.S. Geological Survey Scientific Investigations Report 2008-5200, 69p
- Marfia AM, Krishnamurthy RV, Atekwana EA, Panton WF (2004) Isotopic and geochemical evolution of ground and surface waters in a karst dominated geological setting: a case study from Belize, Central America. *Appl Geochem* 19:937–946
- Marie A, Vengosh A (2001) Sources of salinity in ground water from Jericho Area, Jordan Valley. *Ground Water* 39:240–248
- Martinez R, Sánchez-Mata D, Costa M (1999) Boreal and western temperate forest vegetation (syntaxonomical synopsis of the potential natural plant communities of North America II). *Itiner Geobot* 12: 3–311
- Mehta S, Fryar AE, Banner JL (2000a) Controls on the regional-scale salinization of the Ogallala aquifer, Southern High Plains, Texas, USA. *Appl Geochem* 15:849–864
- Mehta S, Fryar AE, Brady RM, Morin RH (2000b) Modeling regional salinization of the Ogallala aquifer, Southern High Plains, TX, USA. *J Hydrol* 238:44–64
- Ministry of Energy of Iran (2010) Integrated management plan for Lake Urmia Basin. report, 91pp
- Mohammadi K (2012) Optimum management of water extraction from coastal Urmia aquifer. M.Sc. Thesis. Kharazmi University, Tehran (In Persian)
- Mongelli G, Monni S, Oggiano G, Paternoster M, Sinisi R (2013) Tracing groundwater salinization processes in coastal aquifers: a hydrogeochemical and isotopic approach in the Na-Cl brackish waters of northwestern Sardinia, Italy. *Hydrol Earth Syst Sci* 17:2917–2928
- Morrow FJ, Ingham MR, McConchie JA (2010) Monitoring of tidal influences on the saline interface using resistivity traversing and cross-borehole resistivity tomography. *J Hydrol* 389:69–77
- Musgrove M, Fahlquist L, Houston NA, Lindgren RJ, Ging PB (2010) Geochemical evolution processes and water-quality observations based on results of the national water-quality assessment program in the San Antonio Segment of the Edwards Aquifer, 1996–2006. U.S. Geological Survey Scientific Investigations Report 2010-5129, 93p
- NOAA (National Oceanic and Atmospheric Administration). “Oroomieh climate normals 1961–1990”. Retrieved 27 Dec 2012
- Ozturk N, Kavak D, Kose TE (2008) Boron removal from aqueous solution by reverse osmosis. *Desalination* 223:1–9
- Panno SV, Hackley KC, Hwang HH, Greenberg S, Krapac IG, Landsberger S, O’Kelly DJ (2006) Source identification of sodium and chloride in natural waters: preliminary results. *Ground Water* 44:176–187
- Parks JL, Edwards M (2005) Boron in the environment. *Crit Rev Environ Sci Technol* 35(2):81–114
- Prats D, Chillón-Arias MF, Rodríguez-Pastor M (2000) Analysis of the influence of pH and pressure on the elimination of boron in reverse osmosis. *Desalination* 128:269–273
- Ranjan SP, Kazama S, Sawamoto M (2006) Effects of climate change on coastal fresh groundwater resources. *Glob Environ Chang* 16: 388–399
- Ravenscroft P, McArthur JM (2004) Mechanism of regional enrichment of groundwater by boron: the examples of Bangladesh and Michigan, USA. *Appl Geochem* 19:1413–1430
- Reilly TE, Goodman AS (1985) Quantitative analysis of saltwater-freshwater relationships in groundwater systems—a historical perspective. *J Hydrol* 80(1-2):125–160
- Rengasamy P (2006) World salinization with emphasis on Australia. *J Exp Bot* 57:1017–1023
- Riley JP, Skirrow G (eds) (1975) Chemical oceanography. Acad Press, London
- Sagiv A, Semiat R (2004) Analysis of parameters affecting boron permeation through reverse osmosis membranes. *J Membr Sci* 243:79–87
- Samani S, Asghari Moghaddam A (2015) Hydrogeochemical characteristics and origin of salinity in Ajabshir aquifer, East Azerbaijan, Iran. *Q J Eng Geol Hydrogeol*. doi:10.1144/qjegh2014-070
- Schroeder RA, Rivera M (1993) Physical, chemical and biological data for detailed study of irrigation drainage in the Salton Sea area, California. US Geological Survey Open-File report 93-83. Menlo Park, CA: US Geological Survey

- Shamsi A, Kazemi GA (2014) A review of research dealing with isotope hydrology in Iran and the first Iranian meteoric water line. *Geopersia* 4(1):73–86
- Skrzypek G, Dogramaci S, Grierson PF (2013) Geochemical and hydrological processes controlling groundwater salinity of a large inland wetland of northwest Australia. *Chem Geol* 357:164–177
- Sowers J, Vengosh A, Weinthal E (2011) Climate change, water resources, and the politics of adaptation in the Middle East and North Africa. *Clim Chang* 104:599–627
- Sprenger C, Renganayaki SP, Schneider M, Elango L (2015) Hydrochemistry and stable isotopes during salinity ingress and refreshment in surface- and groundwater from the Arani-Koratallai (A-K) basin north of Chennai (India). *Environ Earth Sci* 73(12):7769–7780
- Starinsky A (1974) Relationship between calcium-chloride brines and sedimentary rocks in Israel. PhD Thesis, The Hebrew University
- Stuyfzand PJ (2008) Base-exchange indices as indicators of salinization or freshening of (coastal) aquifers. In *Proceedings of 20th Salt Water Intrusion Meeting*. Florida, June 23–27. pp. 262–265
- Trabelsi R, Abid K, Zouari K, Yahyaoui H (2012) Groundwater salinization processes in shallow coastal aquifer of Djefara plain of Medenine, Southeastern Tunisia. *Environ Earth Sci* 66:641–653
- Tu KL, Nghiem LD, Chivas AR (2011) Coupling effects of feed solution pH and ionic strength on the rejection of boron by NF/RO membranes. *Chem Eng J* 168:700–706
- Vandenbohede A, Van Houtte E, Lebbe L (2009) Water quality changes in the dunes of the western Belgian coastal plain due to artificial recharge of tertiary treated wastewater. *Appl Geochem* 24:370–382
- Vengosh A (1998) The isotopic composition of anthropogenic boron and its potential impact on the environment. *Biol Trace Elem Res* 66:145–151
- Vengosh A (2014) *Treatise on Geochemistry (Second Edition)*. Volume 11: Environmental Geochemistry, 11.9 Salinization and Saline Environments, 325–378 p, doi:10.1016/B978-0-08-095975-7.00909-8
- Vengosh A, Keren R (1996) Chemical modifications of groundwater contaminated by recharge of treated sewage effluent. *J Contam Hydrol* 23:347–360
- Vengosh A, Rosenthal E (1994) Saline groundwater in Israel: its bearing on the water crisis in the country. *J Hydrol* 156:389–430
- Vengosh A, Heumann KG, Juraske S, Kasher R (1994) Boron isotope application for tracing sources of contamination in groundwater. *Environ Sci Technol* 28:1968–1974
- Vengosh A, Barth S, Heumann KG, Eisenhut S (1999a) Boron isotopic composition of freshwater lakes from central Europe and possible contamination sources. *Acta Hydrochim Hydrobiol* 27:416–421
- Vengosh A, Spivack AJ, Artzi Y, Ayalon A (1999b) Geochemical and boron, strontium, and oxygen isotopic constraints on the origin of the salinity in groundwater from the Mediterranean coast of Israel. *Water Resour Res* 35:1877–1894
- Vengosh A, Farber E, Shavit U, Holtzman R, Segal M, Gavrieli I, Bullen TM (2001) Exploring the sources of salinity in the Middle East: a hydrologic, geochemical and isotopic study of the Jordan River. In: Cidu R (ed.) *10<sup>th</sup> International Symposium on Water-Rock Interaction, WRI-10, 2001b Sardinia, Italy*, pp. 71–79. Amsterdam: A.A. Balkema
- Vengosh A, Gill J, Davisson ML, Hudson GB (2002) A multi-isotope (B, Sr, O, H, and C) and age dating ( $^3\text{H}$  -  $^3\text{He}$  and  $^{14}\text{C}$ ) study of groundwater from Salinas Valley, California: hydrochemistry, dynamics, and contamination processes. *Water Resour Res* 38(1):9-1–9-17, 1008
- Vengosh A, Kloppmann W, Marei A, Livshitz Y, Gutierrez A, Banna M, Guerrot C, Pankratov I, Raanan H (2005) Sources of salinity and boron in the Gaza strip: natural contaminant flow in the southern Mediterranean coastal aquifer. *Water Resour Res* 41:W01013
- Vinson DS (2011) Radium isotope geochemistry in groundwater systems: the role of environmental factors. PhD Thesis, Duke University
- Wada Y, van Beek L, van Kempen C, Reckman J, Vasak S, Bierkens M (2010) Global depletion of groundwater resources. *Geophys Res Lett* 37(20). Doi:10.1029/2010gl044571
- Wahi AK, Hogan JF, Ekwurzel B, Baillie MN, Eastoe CJ (2008) Geochemical quantification of semiarid mountain recharge. *Ground Water* 46(3):414–425
- Warner N, Lgourna Z, Boutaleb S, Tagma T, Vinson DS, Ettayfi N, Bouchaou L, Vengosh A (2010) A geochemical approach for the evaluation of water availability and salinity in closed basins: The Draa Basin, Morocco. American Geophysical Union, Fall Meeting, San Francisco
- Warner NR, Jackson RB, Darrah TH, Osborn SG, Down A, Zhao K, White A, Vengosh A (2012) Geochemical evidence for possible natural migration of Marcellus formation brine to shallow aquifers in Pennsylvania. *Proc Natl Acad Sci U S A* 109:11961–11966
- Warner NR, Lgourna Z, Bouchaou L, Boutaleb S, Tagma T, Hsaissoune M, Vengosh A (2013) Integration of geochemical and isotopic tracers for elucidating water sources and salinization of shallow aquifers in the sub-Saharan Drâa Basin, Morocco. *Appl Geochem* 34:140–151
- Williams WD (2001a) Anthropogenic salinisation of inland waters. *Hydrobiologia* 466:329–337
- Williams WD (2001b) Salinization: unplumbed salt in a parched landscape. *Water Sci Technol* 43:85–91
- Williams J, Walker GR, Hatton TJ (2002) Dryland salinization: a challenge for land and water management in the Australian landscape. In: Haygarth PM, Jarvis SC (eds) *Agriculture, hydrology, and water quality*. CAB International, Wallingford
- Wilson TP, Long DT (1993) Geochemistry and isotope chemistry of Ca-Na-Cl brines in Silurian strata, Michigan Basin, U.S.A. *Appl Geochem* 8:507–524
- Wilson SR, Ingham M, McConchie JA (2006) The applicability of earth resistivity methods for saline interface definition. *J Hydrol* 316:301–312
- WMO (World Meteorological Organisation) (2014). <http://worldweather.wmo.int/en/city.html?cityId=1454>
- Zarghami M (2011) Effective watershed management; case study of Urmia Lake, Iran. *Lake Reservoir Manage* 27(1):87–94
- Zarroca M, Bach J, Linares R, Pellicer XM (2011) Electrical methods (VES and ERT) for identifying, mapping and monitoring different saline domains in a coastal plain region (Alt Empordà, Northern Spain). *J Hydrol* 409:407–422
- Zimmerman U, Ehhalt D, Munnich KO (1967) Soil water movement and evapotranspiration: change in the isotopic composition of the water. In: *Isotopes in Hydrology*. IAEA, Vienna p. 567–585